TOWARDS INDIVIDUALIZED DOSAGE ADJUSTMENT OF ANTIMICROBIAL DRUGS USING POPULATION PHARMACOKINETIC MODELING AND SIMULATION

ベラバス, タサディト

TOWARDS INDIVIDUALIZED DOSAGE ADJUSTMENT OF ANTIMICROBIAL DRUGS USING POPULATION PHARMACOKINETIC MODELING AND SIMULATION

2023

Graduate School of Pharmaceutical Sciences, Kyushu University

Department of Clinical Pharmacology and Biopharmaceutics

Tassadit Belabbas

Contents

Abbreviations List

AMR	Antimicrobial resistance
PK	Pharmacokinetics
PD	Pharmacodynamics
TDM	Therapeutic drug monitoring
PPK	Population pharmacokinetics
AUC	Area under the time-concentration curve
MIC	Minimum inhibitory concentration
C_{max}	Peak concentration
C_{min}	Trough concentration
VCM	Vancomycin
MRSA	Methicillin-resistant *Staphylococcus aureus*
PCZ	Posaconazole
IFI	Invasive fungal infection
FN	Febrile neutropenia
HSCT	Hematopoietic cell transplantation
ARC	Augmented renal clearance
ICU	Intensive care unit
CL	Clearance
RRT	Renal replacement therapy
WT	Total body weight
Ccr	Creatinine clearance
ANC	Absolute neutrophils count
CTCAE	Common Terminology Criteria for Adverse Events
PsN	Perl Speaks NONMEM
FOCE–I	First-order conditional estimation method with interaction
IIV	Inter-individual variability
OFV	Objective function value
GOF	Goodness-of-fit
pvcVPC	Prediction- and variability-corrected visual predictive check
DV	Observed concentrations
IPRED	Individual-predicted concentrations
PRED	Population-predicted concentrations
CWRES	Conditional-weighted residuals

CI	Confidence interval
PTA	Probability of target attainment
AML	Acute myeloid leukemia
Vd	Volume of distribution
PTTA	Probability of toxicity target attainment
GVHD	Graft-versus-host disease
MDS	Myelodysplastic syndrome
OS	Oral suspension
DRT	Delayed-release tablet
PPI	Proton pump inhibitor
UGT	Diphospho-glucuronosyltransferase
FDA	Food and Drug Admnistration
AEs	Adverse events
LFT	Liver function test
FIB-4	Fibrosis index
ALBI	Albumin-bilirubin score
AST	Aspartate aminotransferase
ALT	Alanine aminotransferase
ALP	Alkaline phosphatase
TBIL	Total bilirubin
C_{avr}	Average concentration
HR	Hazard ratio
CL/F	Apparent clearance
V/F	Apparent volume of distribution
KA	Absorption rate constant
CMV	Cytomegalovirus
UPLC/MS	Ultra-performance liquid chromatography-mass spectrometry
IS	Internal standard
DMSO	Dimethyl sulfoxide
QC	Quality control
RSD	Relative standard error
LLOQ	Lower limit of quantification
ULOQ	Upper limit of quantification
RT	Room temperature

Introduction

Antimicrobial resistance (AMR) is a growing global health crisis which occurs when microorganisms such as bacteria, viruses, fungi, and parasites develop resistance to antimicrobials drugs, rendering them ineffective in treating infections.[1,2] AMR can affect any person and has the potential to cause significant impact on morbidity, mortality, and healthcare costs, consequent to an increase in the prevalence and burden of infectious diseases.[3-5] The World Health Organization has identified AMR as one of the top 10 global public health threats facing humanity.[1] In addition, it was estimated that 4.95 million deaths were associated with bacterial AMR in 2019, including 1.27 million deaths attributable to antibiotic resistance (Antibacterial and antifungal).[6] This number is predicted to increase to 10 million deaths per year by 2050 if no action is taken.[3]

The overuse and misuse of antibiotics in both humans and animals is believed to be the main factor leading to the emergence of AMR.[7-9] To tackle this crisis, new antibiotics are urgently needed. However, due to the rapid spread of multidrug-resistant germs so called “superbugs”, discovering new drugs has slowed drastically while antimicrobial use is rising.[2] According to the Pew analysis, as of June 2019 only 41 antibiotics were in development, from which only one in four represent a novel drug class or mechanisms of action.[10] Therefore, to address drug resistance, it is imperative to focus on available antibiotics and optimize treatment of effective ones.

Pharmacometrics is a science that uses mathematical models based on pharmacology, biology, physiology, and disease characteristics to understand and predict the pharmacokinetics (PK) and pharmacodynamics (PD) relationships of drugs both in individuals and in populations. PK describe the time course of drug absorption, distribution, metabolism, and excretion, whereas PD describe the relationship between

drug concentration and the observed effect on the organism. Population pharmacokinetic (PPK) approach in pharmacometrics, commonly referred to as nonlinear mixed-effect modeling, allows the study of variability in drug concentration between individuals within a population. [11] In the context of AMR, pharmacometrics can be used to optimize drug dosing regimen and guide drug development, by capturing the dose-exposure relationship.[12-14] Evidence showed the importance of using therapeutic drug monitoring (TDM) based on a PK/PD index obtained from quantitative approaches such as population PPK or PK/PD modeling and simulation to help optimize dosing regimen, maximize efficacy, and minimize the risk of therapeutic failure as well as the risk of toxicity associated with inappropriate use of antimicrobial drugs. Three standard indices are currently used: the time over the 24-h period the free drug concentration remains above the minimum inhibitory concentration (fT >MIC), the ratio of the area under the 24-h time-concentration curve to the MIC (fAUC/MIC), and the ratio of the peak free drug concentration to the MIC (fC_{max}/MIC). [15,16] In addition to the described indices, trough concentration (C_{min}) is often used to assess efficacy and/or occurrence of adverse events. [15] The choice of the PK/PD index or target is based on the antibiotic class and the pathogen target. (Figure 1)

TDM has been widely used in general and special sub-populations However, limited information is available in hematologic malignancies. Thus, the aim of this study was to apply PPK Modeling & Simulation, as well as extensive statistics to hematologic malignancies population to: (1) evaluate the PK and safety of antibiotic drugs, and (2) simulate optimal dosing regimen to maximize efficacy and minimize the risk of therapeutic failure associated with inappropriate use of antimicrobial drugs. The first chapter was dedicated to the development of a PPK model for vancomycin (VCM), a glycopeptide antibiotic frequently used in treating severe bacterial infections caused by gram-positive bacteria, including methicillin-resistant *Staphylococcus aureus*

(MRSA). While the second chapter focused on the development of a PPK model for posaconazole (PCZ), a systemic triazole antifungal indicated in the prophylaxis of invasive fungal infections (IFI) in highly immunocompromised patients.

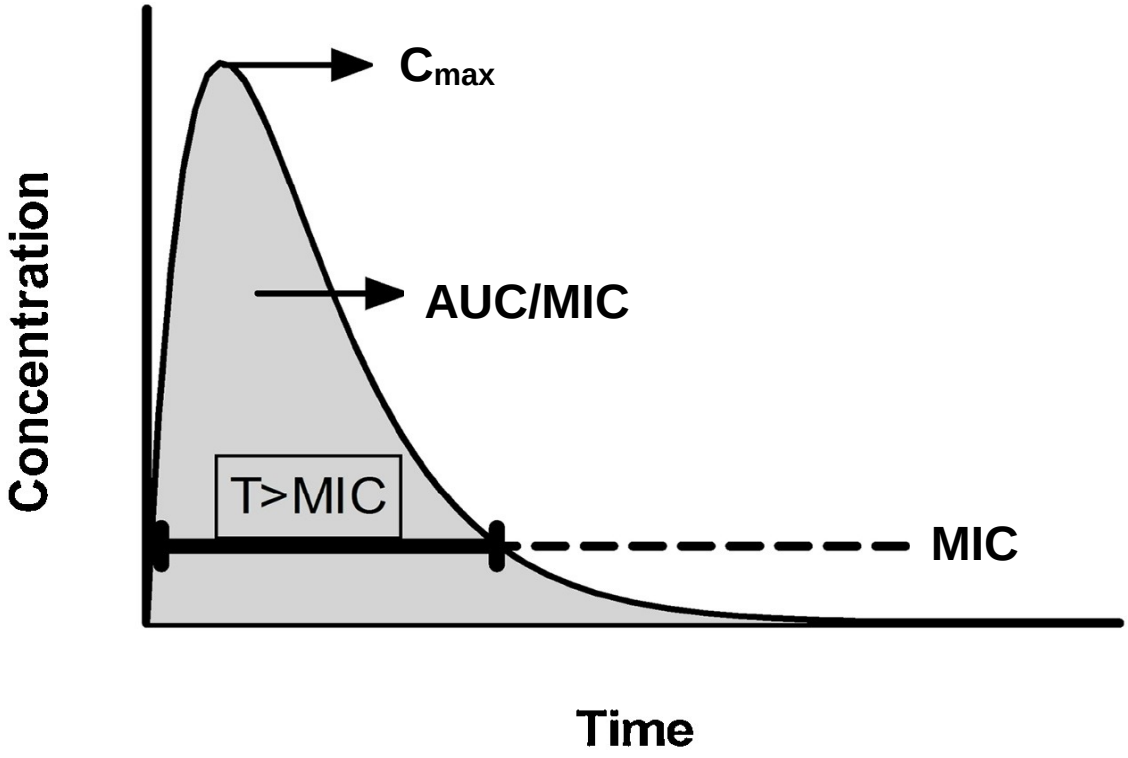

Figure 1. Concentration-time curve showing the standard PK/PD indices used to evaluate safety and efficacy of antimicrobial drugs. The figure was reprinted from the De Velde et al. paper with some modifications [16].

C_{max}, peak concentration; AUC/MIC, the ratio of the area under the time-concentration curve to the minimum inhibitory concentration; T>MIC, the time the drug concentration remains above the minimum inhibitory concentration

Chapter 1 Population pharmacokinetic model and dosing optimization of vancomycin in hematologic malignancies with neutropenia and augmented renal clearance

1. Introduction

VCM is a glycopeptide antibiotic frequently used in treating severe bacterial infections caused by gram-positive cocci, including MRSA. It is commonly initiated as an empirical therapy for febrile neutropenia (FN) occurred in cancer patients.[23] Owing to its narrow therapeutic index, well-established TDM has been widely used for decades. Conventionally, a trough value of 10–20 mg/L has been accepted for optimal dosing safety.[24,25] Instead of measured concentration, new consensus guidelines recommend a AUC_{24} of 400–600 mg·h/L to maximize efficacy and minimize the risk of MIC of 1 mg/L.[17]

Patients with underlying hematologic malignancies, especially those undergoing intensified chemotherapy and hematopoietic cell transplantation (HSCT) are susceptible to various types of microorganisms due to their profound immunocompromised status including severe neutropenia.[23,26-30] It has been reported that FN incidence can be as high as 80% in this population compared to 10%–50% in patients with solid tumors. [23] Thus, pathophysiological changes may occur in patients with hematologic malignancies leading to altered PK parameters.[31-33]In particular, these physiological fluctuations include augmented renal clearance (ARC), which is a phenomenon characterized by enhanced glomerular filtration.[34] Several studies in patients admitted to the intensive care unit (ICU) have identified sepsis, multitrauma, and young age with lower illness severity as potential risk factors for developing ARC.[35-39] ARC has been the topic of numerous studies in the ICU population [34,40-42]

and has been strongly associated with a risk of underexposure to antimicrobial drugs.[36,43,44] However, limited information is available about VCM PK in patients with ARC.[45-47] Additionally, although previous studies have reported that patients with neutropenia or hematologic malignancies exhibit increased VCM clearance (CL_{VCM}),[46,48-50] the effect of neutropenia on CL_{VCM} in patients with hematologic malignancies is still not well understood.

The increased risk of treatment failure due to either suboptimal or elevated concentrations calls for optimization of VCM therapy in patients with hematologic malignancies. According to our preliminary narrative review, no PPK model for a large sample size of hematologic malignancies with concomitant neutropenia and ARC has been described. Moreover, no AUC-based dosing regimen has been proposed to date. Therefore, we aimed to develop a PPK model for VCM in adult patients with hematologic malignancies, evaluate the effect of neutropenia and ARC on the PK of VCM, and propose an optimal dosing regimen.

2. Materials and methods

2.1. A narrative review of VCM PPK analyses

A preliminary narrative review was performed to identify relevant VCM PPK models in various populations. A simple PubMed search was conducted using the following keywords: (vancomycin AND "population pharmacokinetic") OR (vancomycin AND "population pharmacokinetics"). The eligibility criteria included: (1) any described PPK model of VCM; (2) adult subjects; (3) and articles written in English. The exclusion criteria were as follows: (1) studies limited to neonates, infants, and/or children and (2) VCM PK described using a method other than PPK or nonlinear

mixed-effects modeling. Moreover, the references list of the identified articles were thoroughly reviewed to identify any additional relevant studies.

2.2. Study design and population

A retrospective study was conducted on patients with underlying hematologic malignancies treated with VCM for documented or suspected infection with gram-positive bacteria between August 2016 and October 2019. A total of 1237 clinical samples collected for routine TDM from 203 patients were used in the study. Eligible patients included those aged 20 years or older with at least one trough concentration. Patients who had received VCM therapy for less than two days, entered ICU irrespective of renal replacement therapy (RRT), or suffered from severe renal dysfunction on hemodialysis/peritoneal dialysis were excluded. Concentrations below the limit of quantification of 3.0 mg/L were also excluded.

The following data were collected from electronic medical records: gender, age, height, actual body weight (WT), laboratory data, VCM dose regimen, date and time of blood sampling, chemotherapy regimen, and type of underlying hematologic malignancy. Creatinine clearance (Ccr) was estimated using the Cockcroft and Gault formula.[51] ARC was defined as a Ccr value ≥130 mL/min,[36,39] whereas a grade 4 neutropenia was defined as an absolute neutrophil count (ANC) <500 cells/μL, according to the Common Terminology Criteria for Adverse Events (CTCAE) version 5.0.[52]

The study was approved by the Kyushu University Hospital Institutional Review Board (no.2022-39). Informed consent was waived owing to the retrospective nature of the study.

2.3. Measurement of VCM concentration

Serum VCM concentrations were measured using a chemiluminescent immunoassay (ARCHITECT i System, Abbot, Chiba, Japan).[53] The coefficient of variation was <10% for between-day and within-run precision, and the lower limit of quantification was 3.0 mg/L.

2.4. Population pharmacokinetic modeling

Pharmacokinetic analysis was conducted using the non-linear mixed effect modeling system NONMEM® version 7.4.3 (Icon Development Solutions, Ellicott City, MD, USA) in conjunction with Perl Speaks NONMEM (PsN) version 4.9.0 and Pirana version 2.9.9. The first-order conditional estimation method with interaction (FOCE–I) was used throughout the model development. All diagnostic analyses and graphical assessments were performed using Xpose (version 4.7.1) and R software package (version 3.6.3).

2.5. Structural model

Both one- and two-compartment models were considered during model building. Inter-individual variability (IIV) of the PK parameters was evaluated using an exponential model. The residual error model was described using additive, proportional, and combined error models.

2.6. Covariates screening

The effect of Ccr, WT, neutropenia, and type of disease on PK parameters were evaluated with a stepwise forward addition-backward elimination procedure. Covariates were selected based on biological plausibility and statistical significance. Significance was defined as a reduction in the objective function value (OFV) of ≥3.84 (χ^2 distribution with 1 degree of freedom, p <0.05) for the forward addition, and an

increase in the OFV ≥6.64 (χ^2 distribution with 1 degree of freedom, p <0.01) for the backward elimination. Continuous covariates were described with linear, additive, and power models. Additive, proportional, and power models were used to express the relationship between categorical covariates and the typical value of the PK parameters.

2.7. Statistical analysis

Data are presented as mean ± standard deviation. Differences between the two groups were determined using an unpaired student's *t*-test or the non-parametric Mann-Whitney *U* test. Two-way ANOVA was used to compare the effect of two or more independent factors on a continuous variable. Statistical analyses were performed with the R software package. A $p < 0.05$ was considered to be statistically significant.

2.8. Model validation

Model evaluation was based on the goodness-of-fit (GOF) diagnostics and a non–parametric bootstrap with a total of 1,000 resampling with replacement. Lastly, the predictive performance of the final model was evaluated by prediction- and variability-corrected visual predictive check (pvcVPC).[54] A set of 1,000 simulated datasets was created, and the 95% confidence intervals (CI) of the 2.5th, 50th, and 97.5th percentiles of the simulated concentrations were plotted against the observed concentrations.

2.9. Simulation and dose optimization

Using the final developed PPK model, simulations of daily AUC at steady-state (AUC_{ss}) were performed with various VCM dose regimens. To reflect the dataset used for model development, Ccr values in the virtual population created on R software varied from 30 to 180 mL/min. WT was simulated from a bivariate normal distribution.

The AUC_{ss} was calculated as a ratio of the total daily dose to $CL_{VCM.}$ The probability of target attainment (PTA) for each dosing regimen was defined as the proportion of simulated patients in each Ccr group (n = 500) reaching a target AUC_{ss} =

400–600 mg·h/L for efficacy and a target AUC_{ss} >600 mg·h/L for toxicity, at an MIC of 1 mg/L.[17] The optimal dosing regimen achieving the highest PTA while maintaining an acceptable probability of toxicity defined as an AUC_{ss} approximately 500 mg·h/L was selected.

3. Results

3.1. Classification of the previously published VCM PPK models

The flow chart of the narrative review is shown in Figure 2. A total of 75 articles were selected for the final evaluation.

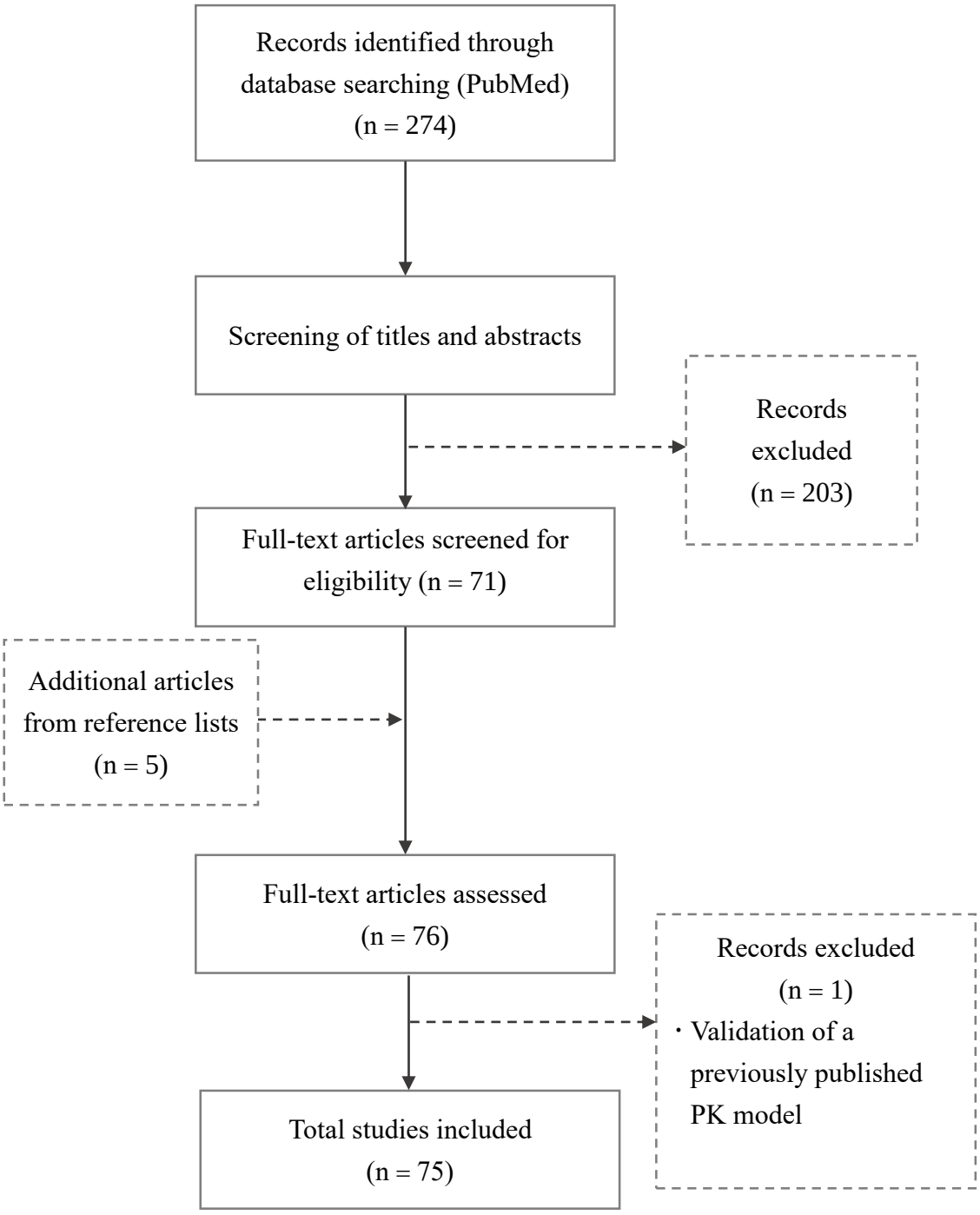

Figure 2. Flow chart describing the narrative review search method

The following data were extracted from the 75 articles: date of publication, population type (including pathology), age, and the modeling approach (nonlinear mixed effect modeling software). All articles were sorted by study population and clinical diagnosis, as described in Figure 3. Of the 75 articles, three articles dealt with hematologic malignancies in the patient population. The current study was classified in the sub-group of hematologic malignancies.

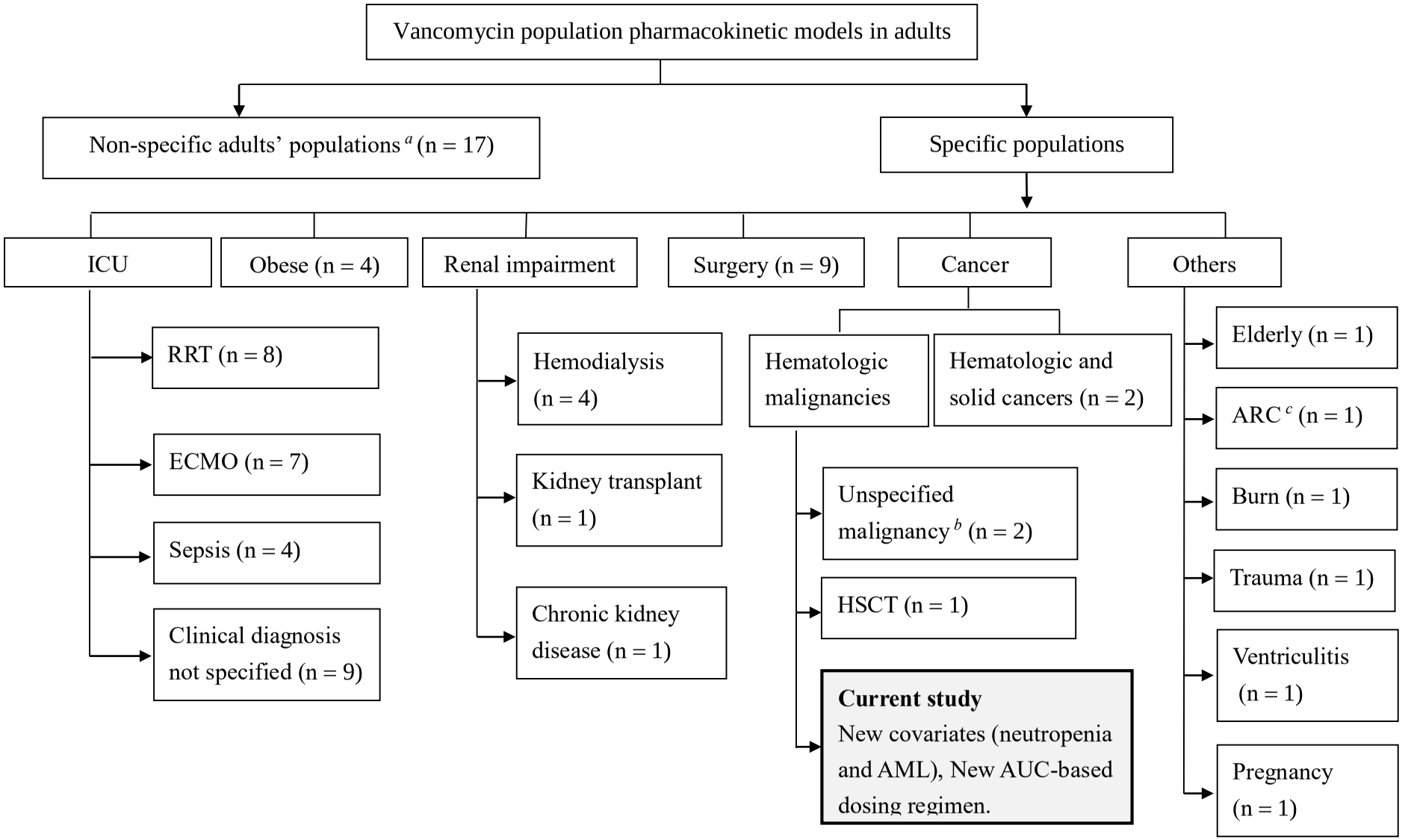
Vancomycin population pharmacokinetic models in adults
Non-specific adults' populations [a] (n = 17)
Specific populations
ICU
Obese (n = 4)
Renal impairment
Surgery (n = 9)
Cancer
Others
RRT (n = 8)
ECMO (n = 7)
Sepsis (n = 4)
Clinical diagnosis not specified (n = 9)
Hemodialysis (n = 4)
Kidney transplant (n = 1)
Chronic kidney disease (n = 1)
Hematologic malignancies
Hematologic and solid cancers (n = 2)
Unspecified malignancy [b] (n = 2)
HSCT (n = 1)
Current study
New covariates (neutropenia and AML), New AUC-based dosing regimen.
Elderly (n = 1)
ARC [c] (n = 1)
Burn (n = 1)
Trauma (n = 1)
Ventriculitis (n = 1)
Pregnancy (n = 1)

Figure 3. Classification of published vancomycin population pharmacokinetic models based on the study population and positioning of the current study. The number in parentheses indicates the number of articles.

[a] Include patients from the general ward or from both intensive care unit and general ward. There was no specific diagnosis mentioned. [b] The study by Fu et al. was limited to patients with grade 4 neutropenia who were 14 years or older. [c] The age range of the population was 11–82 years.

ICU, intensive care unit; RRT, renal replacement therapy; ECMO, extracorporeal membrane oxygenation; HSCT, hematopoietic stem cell transplantation; AML, acute myeloid leukemia; AUC, area under the 24-hour time-concentration curve at steady state; ARC, augmented renal clearance.

3.2. Study population

Patients' baseline demographics and clinical characteristics are presented in Table 2. In total, 681 samples were available from 148 patients (males = 83, females = 65), with a median of four samples per patient (range: 1–17). VCM was administered at a median of 11 days (range: 2–88).

Overall, 57 of 148 (38.5%) patients were diagnosed with acute myeloid leukemia (AML). Ninety-eight (66.2%) patients were on chemotherapy at least 15 days before the initiation of VCM, and 31 (20.9%) patients had sustained chemotherapy during VCM therapy. Additionally, 121 (81.8%) patients were classified as having grade 4 neutropenia. ARC (Ccr value ≥130 mL/min) was observed in 59 (40%) patients. Eleven (7.4%) patients showed moderate renal impairment (Ccr value from 30 to <60 mL/min) and one patient had severe impairment (Ccr value <30 mL/min).

Table 2. Demographics and baseline characteristics

Total (n = 148)	**Mean ± SD or (%)**	**Median [range]**
Age, years	53.6 ± 16.0	59.0 [20.0–82.0]
Sex, n		
Male	83 (56.1)	-
Female	65 (43.9)	-
Body weight, kg	58.7 ± 13.1	57.9 [34.5–105]
Body mass index, kg/m^2	21.7 ± 3.8	21.4 [14.4–33.6]
Serum creatinine, mg/dL	0.6 ± 0.4	0.580 [0.2–5.2]
Creatinine clearance [a], mL/min	122 ± 52.8	112 [12.9–324]
eGFR [b], mL/min/1.73 m^2	110 ± 43.8	101 [10.0–300]
Albumin, g/dL	3.2 ± 0.6	3.30 [1.5–4.5]
Aspartate aminotransferase, U/mL	21.1 ± 16.3	15.5 [5.0–146]
Alanine aminotransferase, U/mL	31.7 ± 34.6	18.0 [3.0–171]
Absolute neutrophils count, × 10^3/μL	0.8 ± 3.0	0.02 [0–27.8]
Neutropenia, n		
Grade 0	14 (9.5)	-
Grade 1	3 (2.0)	-
Grade 2	7 (4.7)	-
Grade 3	3 (2.0)	-
Grade 4	121 (81.8)	-
Underlying malignancies, n		
AML	57 (38.5)	-
ALL	22 (14.9)	-
MDS	10 (6.8)	-
ML	42 (28.4)	-
MM	10 (6.8)	-
Others	7 (4.7)	-

AML, acute myeloid leukemia; ALL, acute lymphoblastic leukemia; MDS, myelodysplastic syndrome; ML, malignant lymphoma; MM, multiple myeloma.

[a] Creatinine clearance was calculated by the Cockcroft and Gault formula [51].

[b] Estimated glomerular filtration rate (eGFR) was calculated by the revised equation for Japanese population [55].

3.3. Population pharmacokinetic modeling

The scatterplot of observed vancomycin concentrations versus time after previous dose is shown in Figure 4. Because the samples analyzed were mostly trough, the peripheral volume of distribution could not be estimated using a two-compartment model. In addition, a relatively high shrinkage was observed for the central volume of distribution, indicating a potential model misspecification. Therefore, the one-compartment model was assumed to better describe VCM data and was preferred for further model development. IIV and residual variability were best described by exponential and additive models, respectively. Whereas, power functions were selected to describe the relationship between potential covariates and VCM PK parameters. Examination of the scatterplots of potential covariates against the empirical Bayes estimates of CL_{VCM} showed a strong correlation between Ccr and CL_{VCM} (Figure 5).

After the forward addition and backward elimination procedure, influential covariates included Ccr, neutropenia, AML on CL_{VCM}, and WT on the volume of distribution (Vd). WT exponent coefficient estimated on Vd was 0.941, consistent with the theoretical allometric coefficient of 1. Therefore, the effect of WT was fixed to 1 in the final model. All parameter estimates and corresponding IIV showed good precision (relative standard error ≤16%) without significant correlation between parameters or covariates.

The following equation describes the model:

$$CL_{TV}\ (L/h) = 3.09 \times (Ccr/90)^{0.988} \times 1.14^{AML} \times 1.09^{Neutropenia} \quad (1)$$

CL_{TV} represents the clearance typical individual value.

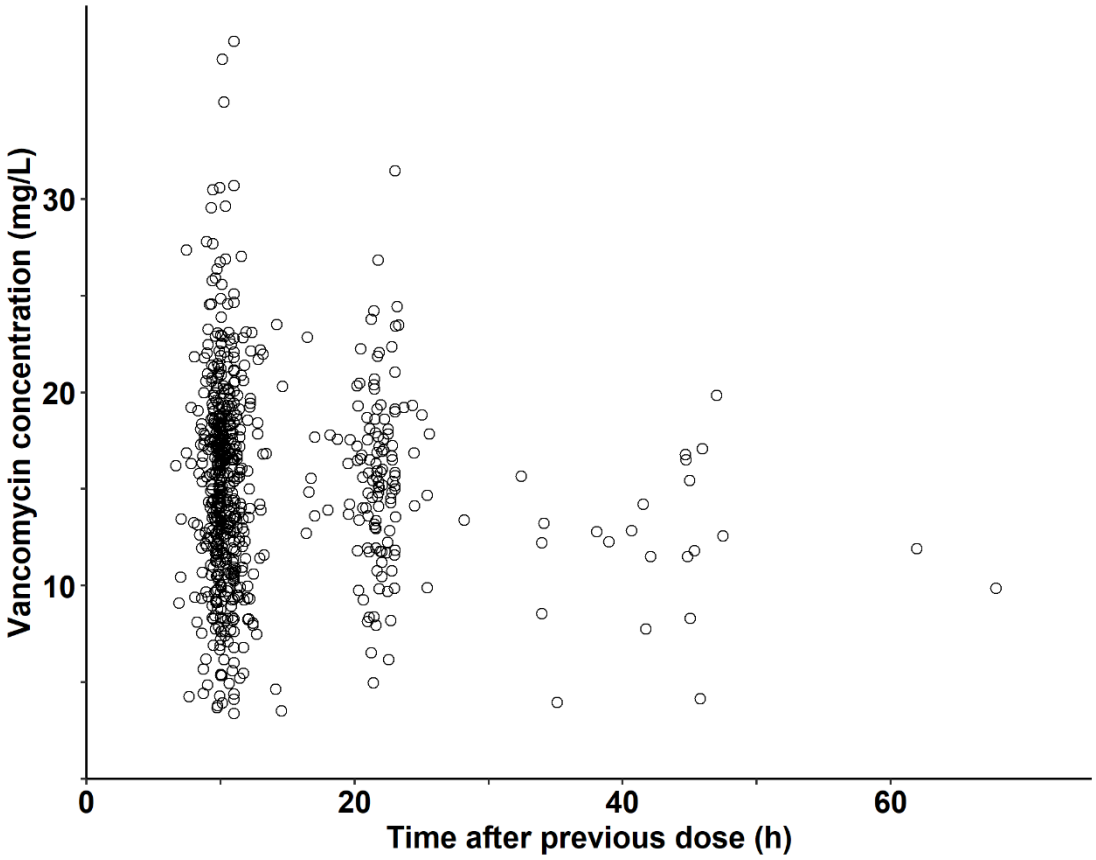

Figure 4. Scatterplot of observed vancomycin concentrations versus time after previous dose.

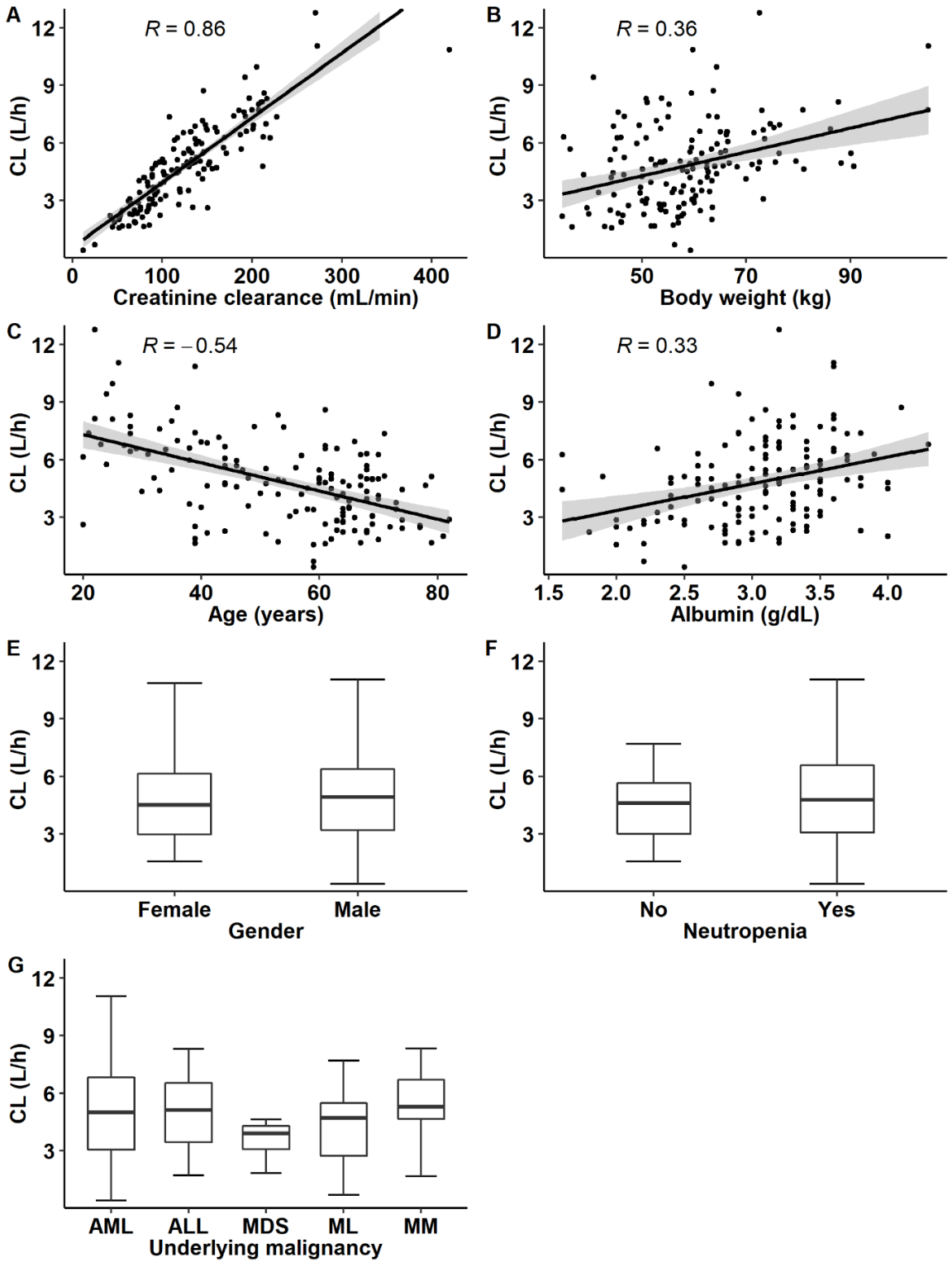

Figure 5. Scatterplots and box plots showing the relationship between the empirical Bayes estimates of vancomycin clearance (CL_{VCM}) and potential continuous and categorical covariates: (A) creatinine clearance, (B) body weight, (C) age, (D) albumin, (E) gender, (F) neutropenia, (G) underlying malignancy. Solid circles represent the individual observed

(CL_{VCM}) (L/h). The solid line in the scatterplots is the linear regression line, while the band is the 95% confidence interval. The middle line in the boxplots represents the median of the distribution. Limits of the box are the first and third quartiles, corresponding to 25^{th} and 75^{th} percentiles, respectively. The lower and upper whiskers represent the minimum and maximum values without outliers.

CL, clearance; AML, acute myeloid leukemia; ALL, acute lymphoblastic leukemia; MDS, myelodysplastic syndrome; ML, malignant lymphoma; MM, multiple myeloma.

To further evaluate the effect of neutropenia and AML on CL_{VCM}, differences in CL_{VCM} in the presence or absence of neutropenia and the presence or absence of AML were described at various levels of renal function (Figure 6).

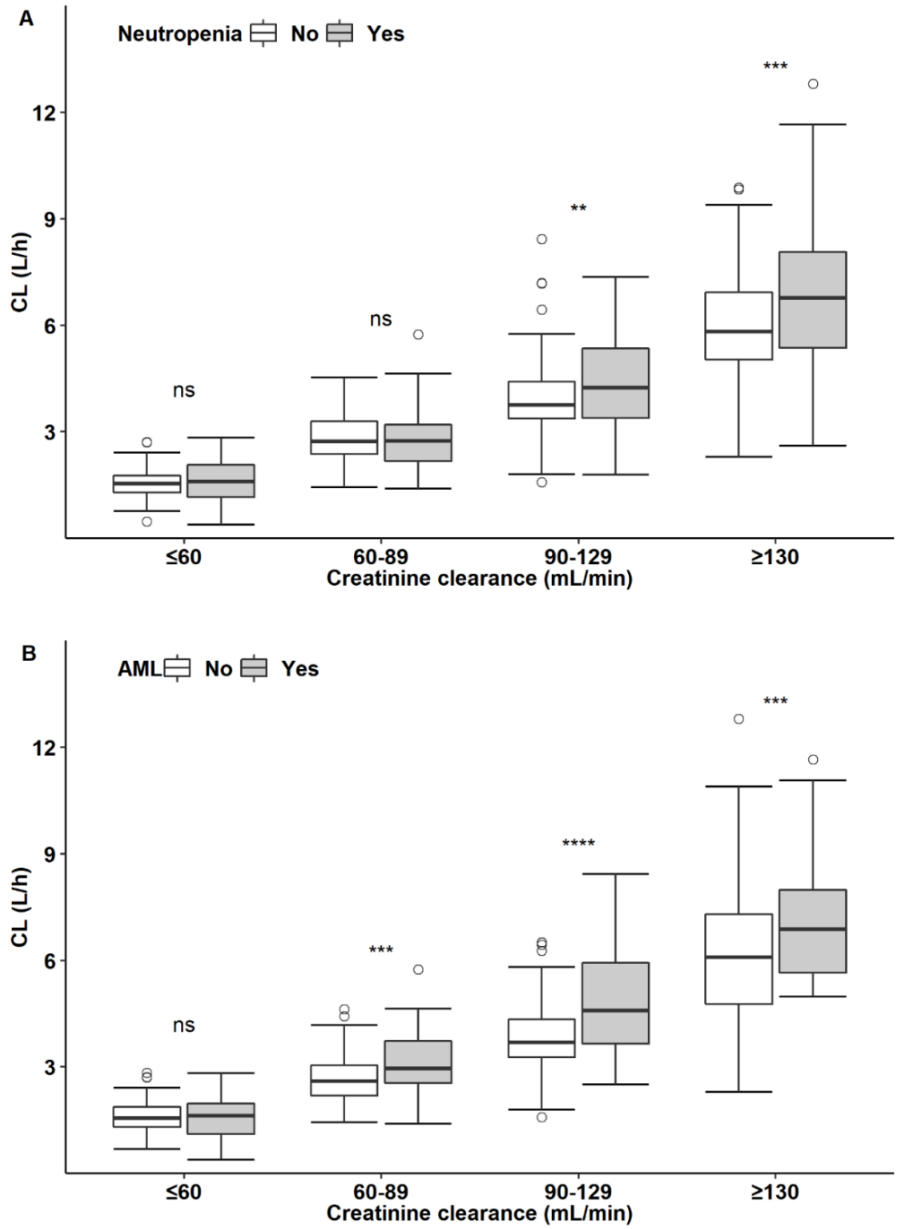

Figure 6. Comparison of vancomycin clearance within different levels of renal function. (A) Neutropenic versus non-neutropenic patients. (B) Acute myeloid leukemia (AML) versus non-AML patients. The middle line represents the median of the distribution. Limits of the box are the first and third quartiles, corresponding to 25th and 75th percentiles, respectively.

The lower and upper whiskers represent the minimum and maximum values without outliers. ns, non-significant, ** p <0.01; *** p <0.001; **** p <0.0001.

A two-way ANOVA revealed that there was a statistically significant interaction between the effects of the Ccr values and neutropenia (F (3), F = 4.05, p = 0.007) and between the effects of the Ccr and AML (F (3), F = 4.49, p = 0.004). An unpaired sample *t*-test was performed to compare CL_{VCM} within each Ccr between neutropenic and non-neutropenic groups and between AML and non-AML patients. We observed a statistically significant difference in CL_{VCM} between AML groups in three out of four Ccr levels (p <0.0001). Conversely, the difference in CL_{VCM} between neutropenic groups was only significant at normal Ccr values (≥90 mL/min), with a lower *p*-value observed within ARC level (p = 0.0005) corresponding to a Ccr value of ≥130 mL/min compared to a Ccr value ranging from 90 to <130 mL/min (p = 0.007). To illustrate the clinical importance of this observation and quantify the effect of neutropenia, the final model was refined by including ARC as a factor for neutropenia. The inclusion decreased OFV by 3.91 points compared to the non-stratified final model. The parameter estimates are presented in Table 3, and the equations for the final model are as follows:

Without ARC (Ccr <130 mL/min):

$$CL_{TV}\,(L/h) = 3.09 \times (Ccr/90)^{0.973} \times 1.15^{AML} \times 1.07^{Neutropenia}$$

With ARC (Ccr ≥130 mL/min):

$$CL_{TV}\,(L/h) = 3.09 \times (Ccr/90)^{0.973} \times 1.15^{AML} \times 1.13^{Neutropenia} \quad (2)$$

$$V_{TV}\,(L) = 122 \times (WT/70)$$

V_{TV} represents the volume of distribution typical individual value

Table 3. Final parameter estimates and bootstrap results

Parameter	Final population estimates		Bootstrap results (n = 1000)*
	Mean (RSE%) [Shrinkage%]	**95% CI**	**Median (95% CI)**
Fixed effects			
CL (L/h),	3.09 (3.2)	2.90–3.28	3.10 (2.90–3.30)
Effect of Ccr on CL	0.973 (4.8)	0.881–1.065	0.969 (0.867–1.060)
Effect of AML on CL	1.15 (4.8)	1.04–1.26	1.15 (1.04–1.26)
Effect of neutropenia on CL			
Without ARC (Ccr <130 mL/min)	1.07 (2.0)	1.03–1.11	1.07 (1.03–1.12)
With ARC (Ccr ≥130 mL/min)	1.13 (3.2)	1.06–1.20	1.13 (1.06–1.20)
V (L/70kg),	122 (7.1)	105–139	122 (105–140)
Effect of WT on V	Fixed to 1	-	Fixed to 1
Inter-individual variability (%CV)			
CL	25.4 (7.6) [9.3]	-	25.1 (21.2–28.8)
V	47.4 (14.2) [30.0]	-	46.6 (30.8–58.1)
Residual variability			
Additive error (mg/L)	4.92 (9.8) [15.3]	-	4.86 (3.95–5.90)

* Success rate was 98.6%

RSE, relative standard error; CI, confidence interval; CV, coefficient of variation; CL, clearance; V, volume of distribution; Ccr, Actual creatinine clearance; AML, acute myeloid leukemia; ARC, augmented renal clearance; WT, actual body weight.

3.4. Model validation

The GOF of the final model are presented in Figure 7 and show acceptable fitting. The results of the bootstrap estimation are summarized in Table 3. The parameter estimates resulting from the bootstrap were similar to their respective values from the final population model. Examination of the pvcVPC plot indicated a good predictive performance of the model, with most observed concentrations falling within the 95% CIs of the simulated values (Figure 8).

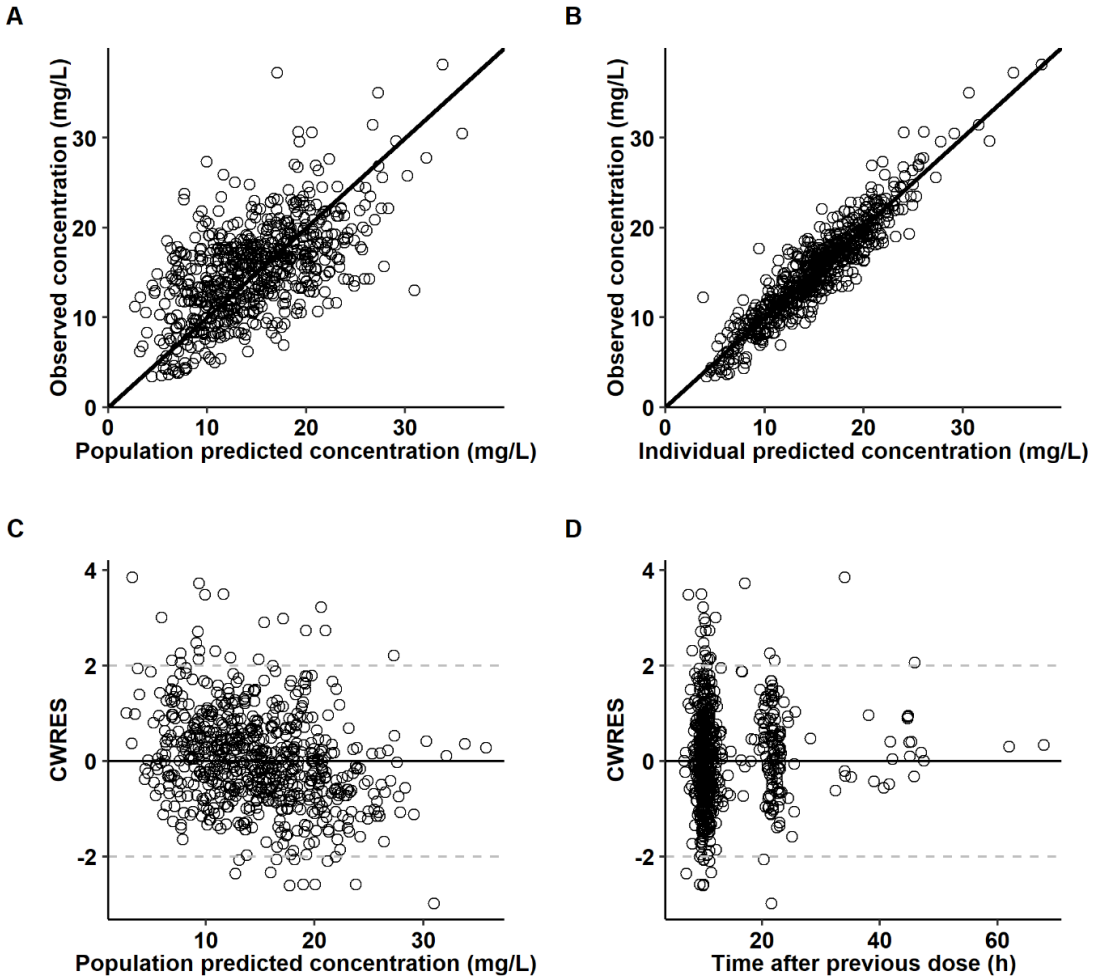

Figure 7. Goodness-of-fit plots for the final population PK model. The solid line represents the line of identity. (A) Observed concentrations (DV) versus population-predicted concentrations

(PRED). (B) DV versus individual-predicted concentrations (IPRED). (C) Conditional-weighted residuals (CWRES) versus PRED. (D) CWRES versus time after the last dose.

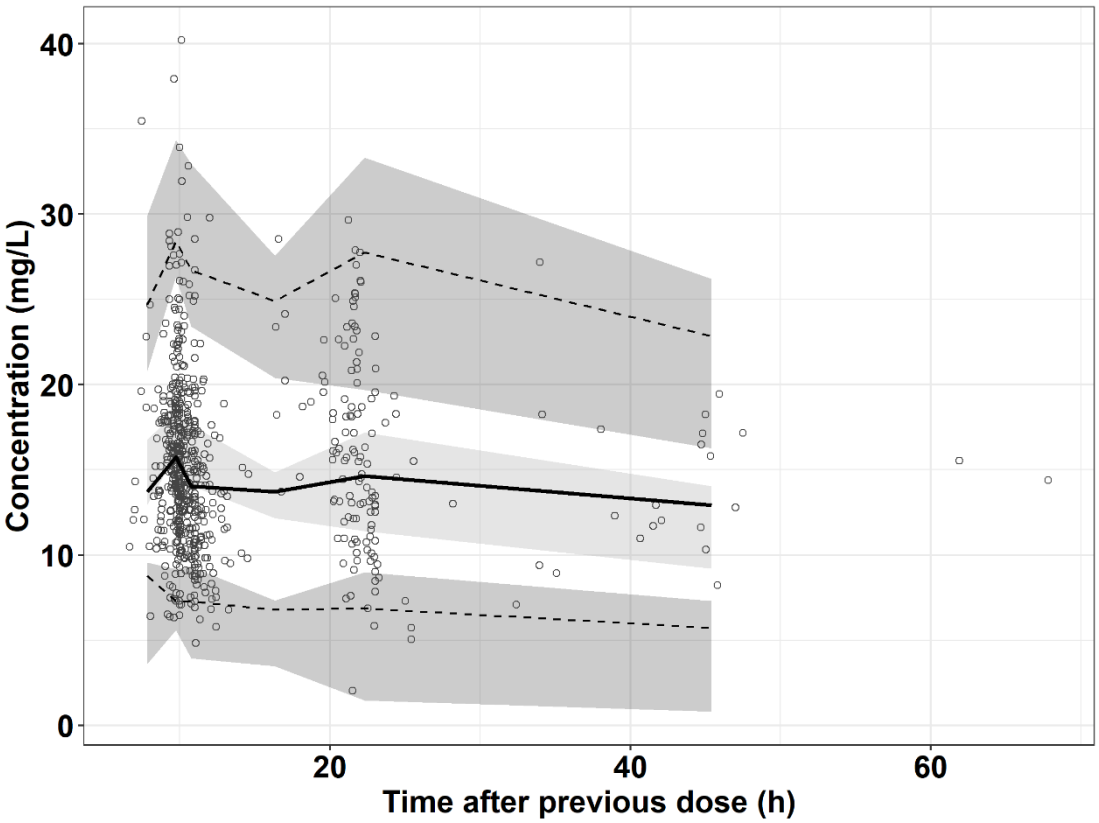

Figure 8. Prediction- and variability- corrected visual predicted check (pvcVPC) of the final population pharmacokinetic model. The open circle represents the prediction-corrected vancomycin concentrations. Shaded areas show the 95% prediction interval of the 2.5th, 50^{th,} and 97.5th percentiles of the simulated values. The solid line indicates the observed median value. The upper and lower dashed lines are the observed 5th and 95th percentile values.

3.5. Simulation and dose optimization

Figure 9 shows the simulated daily AUC_{ss} in different renal function groups in patients with or without neutropenia and/or AML.

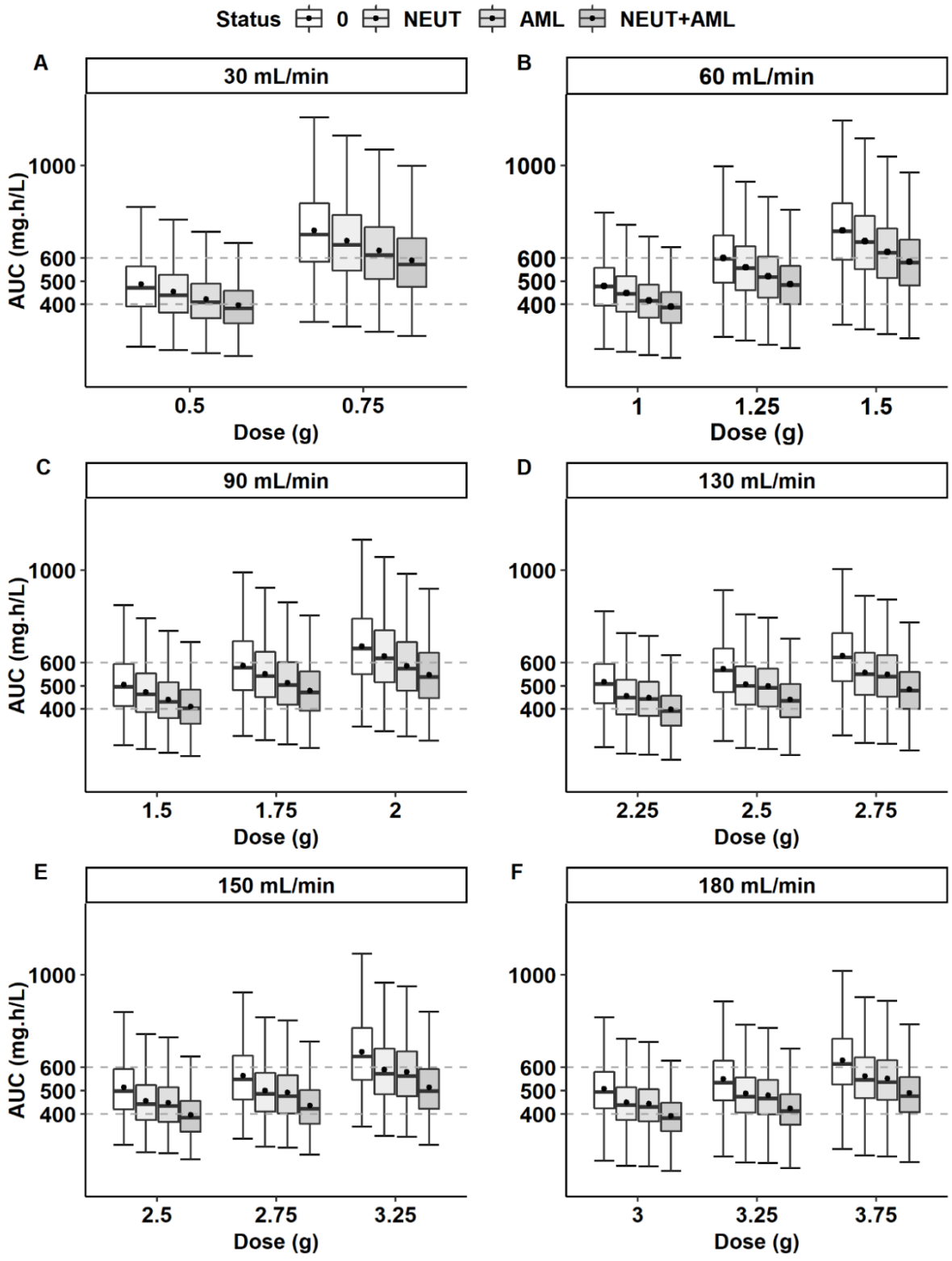

Figure 9. Simulated AUC at steady-state at various dosing regimens in patients with different levels of renal function in the presence or absence of neutropenia and/or acute myeloid leukemia. (A) Creatinine clearance (Ccr) = 30 mL/min. (B) Ccr = 60 mL/min. (C) Ccr = 90 mL/min. (D)

Ccr = 130 mL/min. (E) Ccr = 150 mL/min. (F) Ccr = 180 mL/min. The middle line is the median of the distribution, while the solid circle represents AUC mean. Limits of the box are the first and third quartiles corresponding to 25^{th} and 75^{th} percentiles, respectively. The lower and upper whiskers represent the minimum and maximum values without outliers.

AUC, area under the 24–hour time-concentration curve at steady state; NEUT, neutropenia; AML, acute myeloid leukemia; Factor 0 corresponds to patients without neutropenia and AML.

Based on the simulation results using the final model in different dosing scenarios, the recommended dose regimen to achieve a target AUC_{ss} range of 400–600 mg·h/L at an MIC of 1 mg/L is summarized in Table 4. A. The PTA was between 40.0% and 62.0%, whereas the probability of toxicity target attainment (PTTA) was less than 30.0% for all Ccr values. In patients with normal or moderately impaired renal function, similar doses were observed between neutropenic and non-neutropenic groups, whereas an increase of 0.25 g was necessary for AML patients. Conversely, ARC patients with neutropenia required higher doses compared to ARC patients without neutropenia. A daily dose increase of 30% and 25% was needed among the ARC group to achieve the desired efficacy target in AML patients with neutropenia at Ccr values of 150 mL/min and 180 mL/min, respectively.

Table 4. A Vancomycin recommended dosing regimen in patients with hematologic malignancies for a target AUC at steady state of 400–600 mg·h/L.

Ccr level	Status															
	0 [a]				Neutropenia				AML				Neutropenia+AML			
	Daily dose (g)	Mean AUC_{ss}	PTA (%)	PTTA (%)	Daily dose (g)	Mean AUC_{ss}	PTA (%)	PTTA (%)	Daily dose (g)	Mean AUC_{ss}	PTA (%)	PTTA (%)	Daily dose (g)	Mean AUC_{ss}	PTA (%)	PTTA (%)
30	0.5	487	54.0	18.6	0.5	455	52.0	11.4	0.5	424	46.4	6.6	0.5	396	40.0	4.0
60	1.0	480	57.6	15.2	1.0	448	53.8	8.8	1.25	522	57.4	26.0	1.25	487	57.8	17.4
90	1.5	506	53.4	23.8	1.5	473	54.0	16.0	1.75	514	53.6	25.4	1.75	480	56.0	16.8
130	2.25	519	56.2	24.0	2.5	510	58.6	21.4	2.5	502	58.8	19.4	2.75	488	57.2	18.0
150	2.5	514	57.8	24.0	2.75	500	57.8	20.6	2.75	492	57.2	18.4	3.25	514	57.8	24.0
180	3.0	509	61.0	20.4	3.25	488	62.0	14.6	3.25	479	60.2	14.0	3.75	489	62.0	14.8

Ccr, creatinine clearance; AML, acute myeloid leukemia; $AUC_{ss,}$ area under the 24-hour time-concentration curve at steady state; PTA, probability of target attainment (AUC_{ss} = 400–600 mg·h/L); PTTA, probability of toxicity target attainment (AUC_{ss} >600 mg·h/L).

[a] Factor corresponding to patients without neutropenia and AML.

To further illustrate the clinical impact of the selected final model (equation 2), we performed simulations of the dosing regimen using the PPK model developed without considering ARC as a factor for neutropenia (equation 1) and compared the resulting PTAs and PTTA showed in Table 4. B to the results in Table 4. A. For comparison, we included the results of both recommended dosing regimens obtained using equations 1 and 2.

In the group with creatinine clearance ≥130 mL/min, the vancomycin clearance in the presence of neutropenia derived from equation 1 was less than that derived from equation 2. Thus, higher AUCss values were observed with the same dosing regimen (Table 4. B). However, as a result of the increased exposure, the PTTA increased. Indeed, compared to Table 4. A, a 0.25 g lower dose was selected in patients with neutropenia at Ccr values of 130 mL/min and in AML patients with neutropenia at Ccr values of 150 mL/min and 180 mL/min, considering that the efficacy should be balanced against the risk of nephrotoxicity. Consequently, using equation 1, a 0.25 g lower dose would presumably be recommended for patients with neutropenia at Ccr values of 130 mL/min and AML patients with neutropenia at Ccr values of 150 mL/min and 180 mL/min, considering that the efficacy should be balanced against the risk of nephrotoxicity. Based on the aforementioned points, including ARC in the final model is necessary to optimize the efficacy and minimize the risk of nephrotoxicity in neutropenic patients with ARC.

Table 4. B. Vancomycin dosing regimen in patients with hematologic malignancies for a target AUC at steady state of 400–600 mg·h/L without considering ARC as a factor of neutropenia (Equation 1).

Ccr level	Status															
	0 [a]				Neutropenia				AML				Neutropenia+AML			
	Daily dose (g)	Mean AUC_{ss}	PTA (%)	PTTA (%)	Daily dose (g)	Mean AUC_{ss}	PTA (%)	PTTA (%)	Daily dose (g)	Mean AUC_{ss}	PTA (%)	PTTA (%)	Daily dose (g)	Mean AUC_{ss}	PTA (%)	PTTA (%)
30	0.5	495	53.8	20.2	0.5	454	52.2	11.2	0.5	434	48.6	8.0	0.5	398	40.6	4.4
60	1.0	483	57.8	16.2	1.0	443	53.6	7.6	1.25	529	57.0	28.2	1.25	486	57.4	17.2
90	1.5	506	53.6	23.8	1.5	464	54.2	14.2	1.75	518	53.6	26.0	1.75	475	55.4	16.2
130	2.25	516	57.0	23.0	2.25 [b]	474	54.8	16.0	2.5	503	58.6	19.8	2.75 [b,c]	508	58.6	21.0
					2.5 [c]	526	55.4	26.0								
150	2.5	510	58.2	22.8	2.75 [b,c]	515	58.0	24.0	2.75	492	57.4	18.4	3.0 [b]	492	57.4	18.4
													3.25 [c]	533	57.4	28.0
180	3.0	503	60.6	19.4	3.25 [b,c]	500	61.6	18.0	3.25	478	60.2	13.8	3.5 [b]	473	59.4	12.4
													3.75 [c]	506	60.6	20.2

Ccr, creatinine clearance; AML, acute myeloid leukemia; $AUC_{ss,}$ area under the 24-hour time-concentration curve at steady state; PTA, probability of target attainment (AUC_{ss} = 400–600 mg·h/L); PTTA, probability of toxicity target attainment (AUC_{ss} >600 mg·h/L).

[a] Factor corresponding to patients without neutropenia and AML

[b] Recommended dose using equation 1 (i.e., not considering ARC as a factor of neutropenia).

[c] Same dose as in Table 4. A (i.e., recommended dose using Equation 2).

4. Discussion

We developed a PPK model of VCM and proposed for the first time an optimized dosing regimen in the adult population with hematologic malignancies, based on a target AUC_{ss} = 400–600 mg·h/L at an MIC of 1 mg/L. The current study highlighted the potential impact of neutropenia on the PK of VCM among patients with hematologic malignancies possessing unstable renal function, particularly those with ARC. As sepsis was a known risk factor for developing ARC,[35,36] optimization of VCM dose was critical during severe neutropenia after chemotherapy.

In line with previous studies, we found that neutropenia was a significant covariate on CL_{VCM}. However, the effect in our model was lower as opposed to a recent study by Bury et al. recommending a 25% increase in the dose in patients with neutropenia.[48] This discrepancy may be attributable to different study populations and the incidence and/or severity of neutropenia. In the previous report, the effect of neutropenia (≥grade 2) was quantified in cancer patients including 33% of hematologic malignancies. In contrast, our population consisted only of hematology patients, with approximately 82% having neutropenia grade 4.

The inclusion of ARC as a factor in the final model allowed us to identify subpopulations at risk for sub-therapeutic concentrations in neutropenic patients. The effects of neutropenia on CL_{VCM}, with and without considering ARC, were 1.13 and 1.09, respectively. Although the difference between the two models appeared to be small, the sensitivity analysis results suggested that dose adjustment using the PPK model developed without considering ARC as a factor for neutropenia had a risk of recommending a lower dose and thus reduced therapeutic efficacy in neutropenic patients with ARC. The influence of neutropenia on CL_{VCM} differed among patients with and without ARC, probably due to the stronger correlation between Ccr and CL_{VCM} in the non-ARC group than in the ARC group. A previous study also demonstrated a poor correlation between CL_{VCM} and Ccr in ARC patients compared to non-ARC and non-neutropenic patients.[56] These results suggest that the strong correlation between Ccr and CL_{VCM} might enhance the

competitive effect between renal function and neutropenia, thus decreasing the overall effect of neutropenia on CL_{VCM}.

We found that CL_{VCM} increased by approximately 15% in AML patients, independently of renal function. Furthermore, AML patients with neutropenia required a dose increase up to 30% among the ARC status compared to patients without both risk factors. Our findings suggest that remission induction chemotherapy for AML patients who experience profound myelosuppression, substantial change in general condition, and use multiple other drugs, should be considered at high-risk for suboptimal VCM concentration.

Among hematologic malignancies, AML patients often suffer from severe and prolonged neutropenia, which exacerbate the pre-existing immunocompromised status. Thus, they are further susceptible to recurrent severe infections and subsequent risk of treatment failure. [26,28-30] Significant elevation of inflammatory parameters (e.g., cytokines, ferritin, and C-reactive protein) during an intensive chemotherapy has been observed in some previous studies, which was often associated with a poor prognosis.[57-59] PK in AML patients could be altered as a consequence of the systemic inflammatory response syndrome, secondary to a surge of inflammatory mediators, which leads to a hemodynamic instability characterized by a decrease in vascular resistance and an increase in cardiac output.[60] Indeed, physiological changes subsequent to severe infections have been previously associated with PK variability.[31,33] Our findings of higher CL_{VCM} in AML patients compared to other malignancies provides additional evidence on the potential role of severe infections on drugs PK. However, further studies are warranted to clarify the potential underlying mechanism of AML on drug clearance.

In our study, the typical value of CL_{VCM} was 3.09 L/h (normalized to a Ccr value of 90 mL/min) in the entire cohort, whereas it was 3.80 L/h in AML patients with neutropenia. Okada et al. reported an estimated CL_{VCM} of 4.25 L/h (normalized to a Ccr value of 113 mL/min) in allogeneic HSCT recipients.[61] Other studies in patients with solid cancers [48] or hematological malignancies,[62] demonstrated that the mean value of CL_{VCM} was 3.22 L/h (normalized to Ccr value of 104 mL/min) and 4.99 L/h/70 kg, respectively. Moreover, a comparative study between

patients with hematologic malignancies and non-hematology patients reported CL_{VCM} values of 3.85 L/h/70 kg and 3.57 L/h/70 kg, respectively.[46] Haeseker et al., on the other hand, showed that neutropenic patients exhibited higher CL_{VCM} (4.02 L/h), compared to non-neutropenic patients (3.0 L/h).[50] Although most studies agreed that CL_{VCM} was higher in patients with hematologic malignancies or neutropenia, variability in the reported results was still observed due to the different study populations in the underlying malignancy and different chemotherapy regimens. The volume of distribution in our population (122 L/70 kg) was higher than that described by Buelga et al. in hematological malignancies (74 L/70 kg),[62] but consistent with ICU populations (107 L/70 kg and 118 L/70 kg [63,64]) and Izumisawa et al. (127 L/70 kg), who reported similar results in hematologic malignancies.[46] The higher volume of distribution observed in our population is probably due to the large proportion of patients with ARC.

The present study was limited by the relatively low number of peak levels, which most likely contributed to the difficulty in estimating VCM parameters with a two-compartment model. In addition, the proposed dosing regimen should be used in combination with the conventional TDM method and assessment of serum creatinine level, since renal function fluctuated daily. Another limitation includes the relatively small sample size of non-neutropenic patients, which might underestimate the true effect of neutropenia on CL_{VCM}.

5. Conclusions

We successfully developed a PPK model of VCM and proposed an optimized dosing regimen for the adult population with hematologic malignancies. This novel AUC-based dose regimen can be applied in clinical practice to improve its efficacy while reducing the incidence of nephrotoxicity. We also identified neutropenia and underlying AML as potential risk factors for increased CL_{VCM}. Furthermore, the influence of neutropenia on CL_{VCM} was greater in patients with ARC than in those without ARC. Consequently, neutropenic patients with ARC required higher doses than non-neutropenic patients with ARC, with daily doses ranging from 2.5 to 3.25

g and 2.25 to 3 g, respectively. Our findings provide a better understanding of VCM PK and an optimal strategy for managing these “high-risk” patients in routine clinical practice.

Chapter 2 Pharmacokinetic and safety evaluation of posaconazole delayed-release tablet in hematologic malignancies

1. Introduction

PCZ is an extended-spectrum, systemic triazole antifungal [65] indicated in the prophylaxis of IFI in highly immunocompromised patients, including HSCT recipients who are undergoing high-dose immunosuppressive therapy for graft-versus-host disease (GVHD), and patients receiving remission induction chemotherapy of AML or myelodysplastic syndrome expected to result in prolonged neutropenia.[22,66] PCZ is available in three formulations: an oral suspension (OS), a delayed-release tablet (DRT), and an intravenous injection. [67] Only the DRT and IV formulations are currently approved in Japan.

PCZ OS showed large PK inter- and intra-subject variability. Indeed, its absorption largely depends upon many factors, including food intake, gastric pH, and gastrointestinal motility.[68,69] In addition, studies have reported that the bioavailability of the OS formulation is widely affected by the concomitant administration of proton pump inhibitors (PPIs), histamine-2 (H2) receptor antagonists, or drugs that alter gastric motility such as metoclopramide, as well as the occurrence of mucositis or diarrhea.[70] PCZ is predominately metabolized by uridine diphospho-glucuronosyltransferase (UGT) enzymes, especially UGT1A4. Thereby, co-administration of drugs that can interact with the UGT enzyme, such as phenytoin, rifampicin, and fosamprenavir were also found to increase PCZ CL.[70]

In 2013, the Food and Drug Admnistration (FDA) approved the DRT formulation, a gastro-resistant solid tablet, to overcome the erratic bioavailability commonly associated with the OS. In contrast to the OS, the DRT is believed to be unaffected by gastric acid suppression treatment, or food.[68,71-76] Consequently, PCZ DRT has been proven to result in substantially higher exposure compared to the OS.[72,74,77-79]

Although, several studies demonstrated improved exposure for the DRT over the OS, large variability is still observed.[80-83] For instance, patients with diarrhea,[82,84] mucositis,[76,85] or even obesity [75,81] were associated with a higher risk of underexposure to PCZ DRT. However, limited information is available on the PK of PCZ DRT in clinical setting. Since the approval of the DRT formulation, only three populations PK models using real world data have been reported so far.[85-87]

PCZ DRT is considered to be safe and well tolerated, despite higher concentrations.[68,71,74,88-90] Initial safety analyses suggest that the treatment-related adverse-events (AEs) commonly observed with the DRT were similar to those with PCZ OS, and mainly include diarrhea, and headache.[71,73,77] However, few studies have described elevations of liver function tests (LFTs) in real life setting. The reported LFTs abnormalities were mostly moderate and varied between 15-20%.[80,90,91] Although cases of PCZ resulting in liver injury have been documented, to the best of our knowledge there is currently no association between PCZ exposure and the occurrence of hepatotoxicity.

In light of these finding, additional studies are warranted to better understand the PK and safety of PCZ DRT in hematologic malignancies. Therefore, the main objectives of this study were to (1) develop a PPK model and explore influential covariates; (2) determine the incidence of hepatotoxicity in Japanese population with hematologic malignancies, and explore potential relationship between PCZ DRT exposure and the risk of hepatotoxicity.

2. Material and methods

2.1. Study design and population

A retrospective study was conducted on patients with underlying hematologic malignancies who received PCZ DRT for prophylaxis or treatment between July 2021 and November 2022. PCZ was orally administered as Noxafil® tablets with a starting loading dose of 300 twice a day on the first day of treatment, followed by a maintenance dose of 300 mg once a day thereafter. The loading dose, as well as the maintenance dose were adjusted at the discretion of the physician. Eligible criteria included: (1) adult patients aged 20 year or older who received PCZ for a minimum of five consecutive days, (2) hospitalized patients with underlying hematologic malignancies, (3) patients with at least one measured concentration obtained within 30 days following the initiation of PCZ therapy for the PPK analysis, and at least one steady-state observation (≥5 days) for the safety evaluation. ICU patients, and patients on RRT were excluded from the study.

Baseline characteristics and clinical data were obtained retrospectively from electronic medical records. For all patients, clinical data were available until hospital discharge, discontinuation, or loss of follow up. PCZ dosing information and sampling time, concomitant medication, AEs, and reason for therapy discontinuation were also obtained.

Previously published cutoffs were used for fibrosis classification (FIB-4 index). FIB-4 values <1.30, between 1.30 and 2.67, and over 2.67 were considered as low, intermediate, and high risk, respectively.[92] Albumin-bilirubin (ALBI)score on the other hand was defined as follow: grade 1, 2, and 3 = ≤-2.60, >-2.60 to -1.39, and >-1.39, respectively. [93,94] In addition, diarrhea was defined as a stool type 6 or higher, according to the Bristol stool form scale. [95]

The study was approved by the Kyushu University Hospital Institutional Review Board (no. 22204-00). If the stored residual samples were used to measure PCZ concentrations, informed consent was waived owing to the retrospective nature of the study.

2.2. Measurement of PCZ concentration

The serum was separated by centrifugation (3000 rpm for 10 min) and stored below - 20℃ until measurement, and for a maximum of one month.

PCZ serum concentrations were measured by a developed and validated LC/MS bioanalytical method. Samples were prepared using a simple protein precipitation method. Separation was performed in reverse phase mode using an ACQUITY UPLC BEH C18 column (Waters, Milford, MA, USA, 130 Å, 1.7 µm, 2.1 mm × 50 mm) maintained at 50°C, coupled with an ACQUITY® QDa detector (Waters, Milford, MA, USA). The mobile phase was delivered at a flow rate of 0.4 mL/min through gradient elution and consisted of 0.1% formic acid (aqueous mobile phase A), and acetonitrile (organic mobile phase B). The injection volume was 1 µL, and the run time was 5.6 min.

The method was validated according to the FDA guidelines on bioanalytical method development and validation in terms of linearity, accuracy, precision, selectivity, carry-over, matrix effect, recovery, and stability. The method was linear over a range of 0.2–10 mg/L (R^2 >0.99). Accuracy and precision of the QCs varied from 99% to 106%, and from 1.7% to 4.5%, respectively. The specificity, recovery, matrix effect, and stability of the method were also within acceptable limits.

2.3. Population pharmacokinetic modeling

PPK analysis was performed using non-linear mixed effect modeling system NONMEM® version 7.4.3 (Icon Development Solutions, Ellicott City, MD, USA) aided with PsN version 5.3.0, and Pirana version 2.9.9 as a graphical interface. The FOCE–I was used for parameter estimation. Data processing, diagnostic analyses and graphical assessments were performed using Xpose (version 4.7.1) and R software package (version 4.2.2).

2.4. Structural model

Various alternative models were assessed to identify the best structural model, including one-compartment and two-compartment models, with either a sequential-zero order and first order absorption, or a first-order absorption. IIV of the PK parameters was evaluated using an exponential model given by the following equation:

$$P_i = \theta_{TV} \times e^{\eta i}$$

Where P_i is the PK parameter of the ith individual, θ_{tv} is the typical value of the parameter in the population and ηi is the inter-individual random effect following a normal distribution with mean of zero and variance ω_i^2.

Residual error model was initially described with a combined error model:

$$Y_{ij} = F_{ij} \times (1 + \varepsilon_{pro,i,j}) + \varepsilon_{add,i,j}$$

Y_{ij} and F_{ij} are observed and predicted concentration for individual i at the time point j, respectively. $\varepsilon_{pro,ij}$ and $\varepsilon_{add,ij}$ are proportional and additive residual errors flowing a normal distribution with mean zero and variance σ^2_{pro} and σ^2_{add}, respectively.

2.5. Covariates screening

Covariates screening was performed with a stepwise forward addition-backward elimination procedure. Covariates were selected based on biological plausibility, statistical significance, and clinical relevance. Significance was defined as a reduction in the OFV of ≥3.84 (χ^2 distribution with 1 degree of freedom, p <0.05) for the forward addition, and an increase in the OFV ≥6.64 (χ^2 distribution with 1 degree of freedom, p <0.01) for the backward elimination. In addition, a 95% CI not including the null value, a reduction in the IIV, and clinical relevance were also considered. Candidate covariates tested included: age, WT, sex, disease type (underlying malignancy, transplantation), Ccr, fasting status, diarrhea, hepatic function (aspartate aminotransferase (AST), alanine aminotransferase (ALT), alkaline phosphatase (ALP), total bilirubin (TBIL), FIBI score, FIB-4 index, ALBI score/grade), and concomitant PPI or steroids.

Continuous covariates were described with linear, additive, and power models. Additive, proportional, and power models were used to express the relationship between categorical covariates and the typical value of the PK parameters.

2.6. Model evaluation

Model evaluation was performed based on the GOF, including observed concentrations (DV versus population-predicted concentrations (PRED), DV versus individual-predicted concentrations (IPRED), and conditional-weighted residuals (CWRES) versus PRED. Stability and robustness of the final model was assessed using a non–parametric bootstrap with a total of 1,000 resampling with replacement. Additionally, Lastly, the predictive performance of the final model was evaluated by prediction-corrected visual predictive check (pcVPC).[54] A set of 1,000 simulated datasets was created, and the 95% CI of the 2.5th, 50th, and 97.5th percentiles of the simulated concentrations were plotted against the observed concentrations

2.7. Simulation

Simulations were carried out using the final PPK model to investigate the PTA, following a dose 300 mg for one week. Target was defined as a trough ≥ 0.7 mg/L for prophylaxis.[96] In addition, the effects of identified covariates on the PK profile of PCZ were assessed by varying one covariate at a time, while maintaining other covariates at a reference level (median). For continuous covariates, different levels consisted of the 5^{th}, 50^{th}, and 95^{th} percentiles of the population distribution. For each scenario, 1000 virtual subjects were simulated.

2.8. Safety assessment

PCZ safety was assessed based on LFTs following PCZ administration. LFTs (TBIL, AST, ALT, and ALP) levels were obtained before PCZ therapy and during the follow-up period limited to 28 days. The hepatotoxicity was defined as an elevation of at least one LFT, defined as per the

CTCAE guidelines (Table 5).[52] Increase of baseline LTFs levels to a grade I or higher was considered.

Average PCZ steady-state trough concentration (C_{avr}) obtained before the occurrence of the event, or until the end of the follow-up period, was used to evaluate the relationship between PCZ exposure and the probability of developing hepatotoxicity. For patients without steady-state concentration, the predicted concentration obtained from the validated PPK model was used instead.

The primary endpoint of the safety assessment was to evaluate the incidence of hepatotoxicity following PCZ therapy in hematologic malignancies and explore potential correlation with PCZ exposure. Secondary outcome was the identification of associated risk factors for developing hepatotoxicity.

Table 5: The Common Terminology Criteria for Adverse Event Grade Scores for Liver Function Tests

Baseline <ULN				
LFT	Grade			
	1	2	3	4
AST	> ULN–3.0 × ULN	> 3.0–5.0 × ULN	> 5.0–20.0 × ULN	> 20.0 × ULN
ALT	> ULN–3.0 × ULN	> 3.0–5.0 × ULN	> 5.0–20.0 × ULN	> 20.0 × ULN
ALP	> ULN–2.5 × ULN	> 2.5–5.0 × ULN	> 5.0–20.0 × ULN	> 20.0 × ULN
TBIL	> ULN–1.5 × ULN	> 1.5–3.0 × ULN	> 3.0–10.0 × ULN	> 10.0 × ULN
Baseline >ULN				
LFT	Grade			
	1	2	3	4
AST	1.5–3.0 × Baseline	> 3.0–5.0 × Baseline	> 5.0–20.0 × Baseline	> 20.0 × Baseline
ALT	1.5–3.0 × Baseline	> 3.0–5.0 × Baseline	> 5.0–20.0 × Baseline	> 20.0 × Baseline
ALP	1.5–3.0 × Baseline	> 3.0–5.0 × Baseline	> 5.0–20.0 × Baseline	> 20.0 × Baseline
TBIL	> 1.0–1.5 × Baseline	> 1.5–3.0 × Baseline	> 3.0–10.0 × Baseline	> 10.0 × Baseline

LFT, Liver function test; AST, aspartate aminotransferase; ALT, alanine aminotransferase; ALP, alkaline phosphatase; TBIL, total bilirubin; ULN, Upper Limit of Normal: TBIL = 1.5 mg/dL, AST = 30 U/mL, ALT = 42 U/mL for males and 23 U/mL for females, ALP = 113 U/mL

2.9. Statistical analysis

Kaplan-Meier plot was used to estimate the probability of developing hepatotoxicity at different time points over 28 days. Patients were censored if they were discontinued, discharged, or did not show any sign of hepatotoxicity before the cutoff time of 28 days.
Additionally, a Cox regression analysis was performed to estimate the hazard ratio (HR) and its corresponding 95% CI for each predictor variable. Univariate analysis was first conducted to identify any significant predictors of hepatotoxicity. Variables with p-values less than 0.05 were considered significant and were included in the multivariate analysis. Multivariate analysis was then carried out to identify risk factors associated with hepatotoxicity after adjusting for other covariates. Analyses were performed with the R software package.

3. Results

3.1. Patients' demographics and clinical data

A total of 131 observations from 26 patients (males =17, females =9) were included in the analysis, ranging from one to 14 measurements per patient with a median of five measurements. The demographic and baseline characteristics of the population are represented in Table 6.
23 patients (88.5%) received PCZ for prophylaxis, and most of the patients received concomitant PPI (96.2%), and steroids (80.8%). Regarding the underlying malignancy, 10 patients (38.5%) were diagnosed with AML, against 19.2% with MDS. Diarrhea was observed in eight patients (30.8%).

Table 6. Demographics and baseline characteristics

Total (n = 26)	**Mean ± SD or (%)**	**Median [range]**
Age, years	49.4 ± 17.3	53.5 [21.0–78.0]
Sex, n		
Male	17 (65.4%)	-
Female	9 (34.6%)	-
Body weight, kg	56.5 ± 13.4	55.4 [35.8–84.6]
Body mass index	20.3 (3.61)	19.5 [13.1–26.7]
Serum creatinine, mg/dL	0.852 ± 0.337	0.805 [0.270–1.84]
Total proteins	5.3 ± 0.818	5.4 [3.90–7.10]
Creatinine clearance [a], mL/min	94.5 (66.8)	74.8 [31.3–363]
Albumin, g/dL	3.28 ± 0.527	3.35 [1.90–4.00]
Protein C reactive (mg/dL)	0.568 ± 1.20	0.110 [0.0100–5.98]
Total bilirubin	0.750 ± 0.437	0.60 [0.30–1.90]
Aspartate aminotransferase, U/mL	23.2 ± 9.88	21.0 [8.0–46.0]
Alanine aminotransferase, U/mL	38.3 ± 27.6	32.0 [5.0–109]
Alkaline phosphatase (U/mL)	107 (51.9)	96.0 [57.0–289]
Gamma-glutamyltransferase (U/mL)	120 (136)	76.5 [14.0–516]
ALBI score	-2.09 (0.489)	-2.21 [-2.73–0.700]
ALBI grade, n		
Grade 1 (ALBI score ≤ −2.60)	3 (11.5%)	-
Grade 2 (−2.60< ALBI score ≤ −1.39)	21 (80.8%)	-
Grade 3 (ALBI score > −1.39)	2 (7.7%)	-
Fibrosis (FIB)-4 index	5.50 (6.59)	2.95 [0.530–30.1]
FIB-4 index grade, n		
Low risk (FIB-4 index < 1.3)	1 (3.8%)	-
Intermediate (FIB-4 index 1.30–2.67)	9 (34.6%)	-
High risk (FIB-4 index > 2.67)	16 (61.5%)	-
Absolute neutrophils count, × 10^3/μL	3.45 (3.14)	2.36 [0.0100–12.1]
Indication, n		
Prophylaxis	23 (88.5%)	-
Treatment	3 (11.5%)	-

Total (n = 26)	**Mean ± SD or (%)**	**Median [range]**
Diarrhea		
Presence	8 (30.8%)	
Absence	18 (69.2%)	
Neutropenia, n		
Grade 0	21 (80.8%)	-
Grade 1	0 (0%)	-
Grade 2	1 (3.8%)	-
Grade 3	0 (0%)	-
Grade 4	4 (15.4%)	-
Underlying malignancies, n		
Acute myeloid leukemia (AML)	10 (38.5%)	-
Myelodysplastic syndrome (MDS)	5 (19.2%)	-
Acute lymphocytic leukemia (ALL)	5 (19.2%)	
Others	6 (23.1%)	-
HSCT, n	21 (80.8%)	-
Concomitant medication, n		
Proton pump inhibitor (PPI)	25 (96.2%)	-
Steroids	21 (80.8%)	-

ALBI, albumin-bilirubin grade; AML, acute myeloid leukemia; ALL, acute lymphoblastic leukemia; MDS, myelodysplastic syndrome; ML, chronic myeloid leukemia; HSCT, hematopoietic stem cell transplantation; GVHD, graft versus host disease.

[a] Creatinine clearance was calculated by the Cockcroft and Gault formula.

3.2. Population pharmacokinetic modeling

A one-compartment model with a first-order absorption adequately described PCZ data. No difference in the model fit was observed between the sequential zero-order and first-order absorption, and the first-order absorption models. Therefore, the latter was selected to avoid over parametrization. The final structural model was parameterized in terms of apparent clearance (CL/F), apparent volume of distribution (V/F), and absorption rate constant (KA). Due to the lack of blood samples at the initial absorption phase, estimate of KA was fixed to previously reported value.[97]

The IIV and residual variability were best described with an exponential model and proportional error model, respectively.

Following stepwise-forward addition and backward elimination, statistically significant covariates included diarrhea, total proteins, sex, and FIB-4 grade 3 on CL/F. However, in the full covariates model, 95% CI for the effect of sex and FIB-4 grade 3 included null values. Therefore, only diarrhea and total proteins were retained in the final model. The final model was stabilized by the inclusion of WT on both CL and V with allometric scaling. The final parameter estimates are presented in Table 7. All parameter estimates and corresponding IIV showed good precision (RSE <25%) without significant correlation between parameters. Additionally, the η-shrinkage for IIV on CL, and ε-shrinkage (proportional error) were both <16%.

The following equations describe the final model:

$$CL_{TV}\ (L/h) = 7.57 \times (WT/70)^{0.75} \times 1.26^{Diarrhea} \times (Total\ proteins/5.4)^{-1.40}$$

$$V_{TV}\ (L) = 296 \times (WT/70)$$

CL_{TV} represents the apparent clearance typical individual value, while V_{TV} represents the apparent volume of distribution typical individual value.

Total proteins variable was centered around the median value 5.4 g/dl.

3.3. PPK model evaluation

The goodness-of-fit plots of the final model are presented in Figure 10 and show acceptable fitting. As shown in Figure 10A and B, the PRED and IPRED were evenly distributed around the line of unity. Figure 10C and D show an equal distribution of the CWRES around the zero line, with the majority of points lying within the range –2 and +2. Examination of the pcVPC plot indicated a good predictive performance of the model, with most observed concentrations falling within the 95% CIs of the simulated values (Figure 11).

The parameter estimates resulting from the bootstrap (Table 7) were similar to their respective values from the final population model, demonstrating the stability of the model.

Table 7. Final parameter estimates and bootstrap results for posaconazole population

Parameter	Final population estimates		Bootstrap results (n = 1000)*
	Mean (RSE%) [Shrinkage%]	**95% CI**	**Median (95% CI)**
Fixed effects			
CL/F (L/h/70kg),	7.54 (7.5)	6.43–8.65	7.53 (6.20–8.73)
Diarrhea on CL	1.26 (7.1)	1.08–1.44	1.24 (1.02–1.48)
Total proteins on CL	-1.4 (28.4)	-2.18–-0.62	-1.17 (-1.92–-0.34)
V/F (L/70kg),	296 (17.6)	194–398	271 (172–381)
KA (h^{-1}),	Fixed to 0.853	-	-
Inter-individual variability (%CV)			
CL	33.5 (18.9) [15.5]	-	32.7 (14.1–44.3)
V	69.1 (21) [23.9]	-	61.2 (20.4–90.5)
Residual variability			
Proportional error (CV%)	18.4 (15.1) [13.8]	-	17.9 (14.2–21.056)

*Success rate was 95.8%

RSE, relative standard error; CI, confidence interval; CV, coefficient of variation; CL/F, apparent clearance; V/F, apparent volume of distribution; KA, absorption rate constant

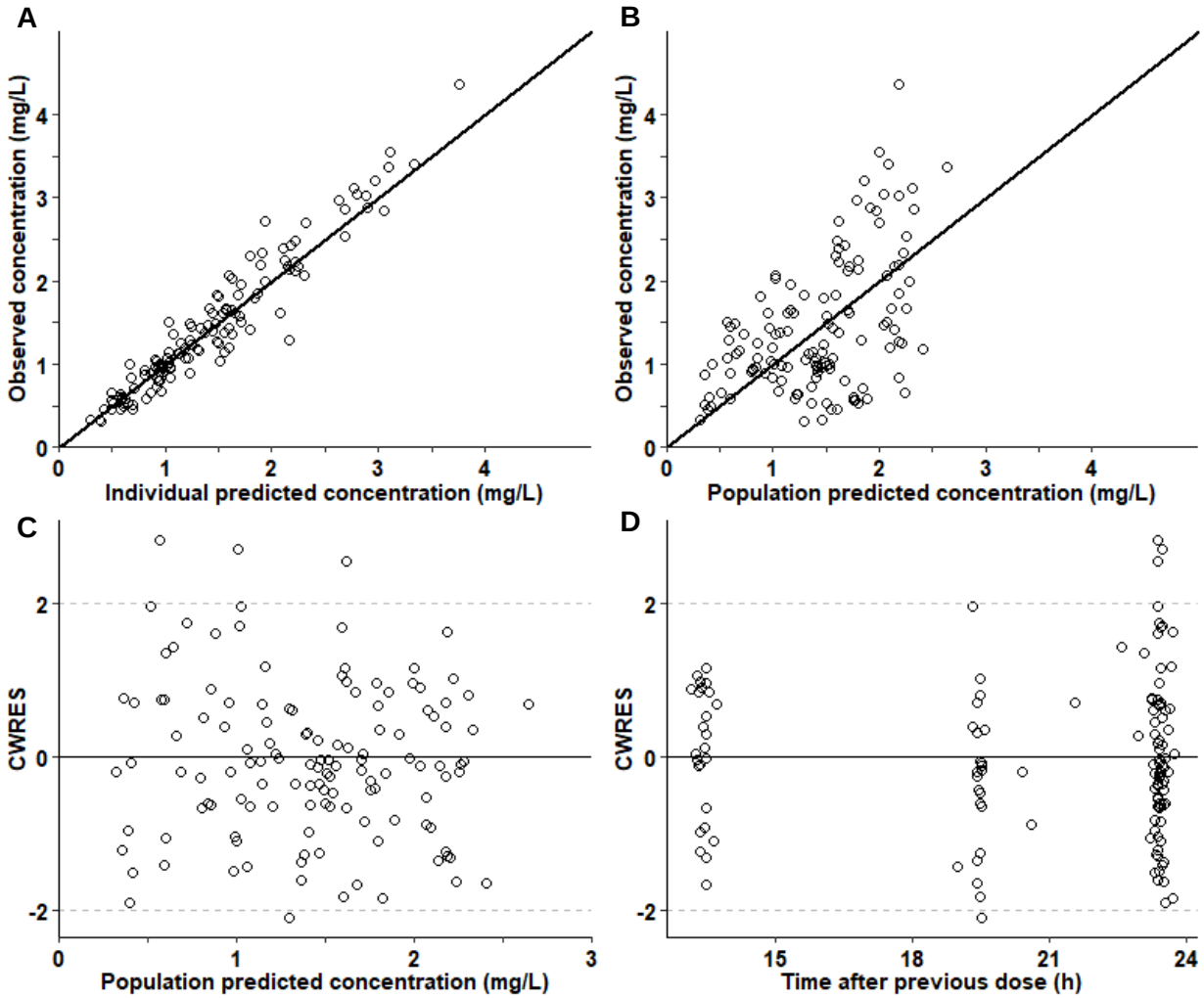

Figure 10. Goodness-of-fit plots for the final population PK model. The solid line represents the line of identity. (A) Observed concentrations (DV versus population-predicted concentrations (PRED). (B) DV versus individual-predicted concentrations (IPRED). (C) Conditional-weighted residuals (CWRES) versus PRED. (D) CWRES versus time after the last dose

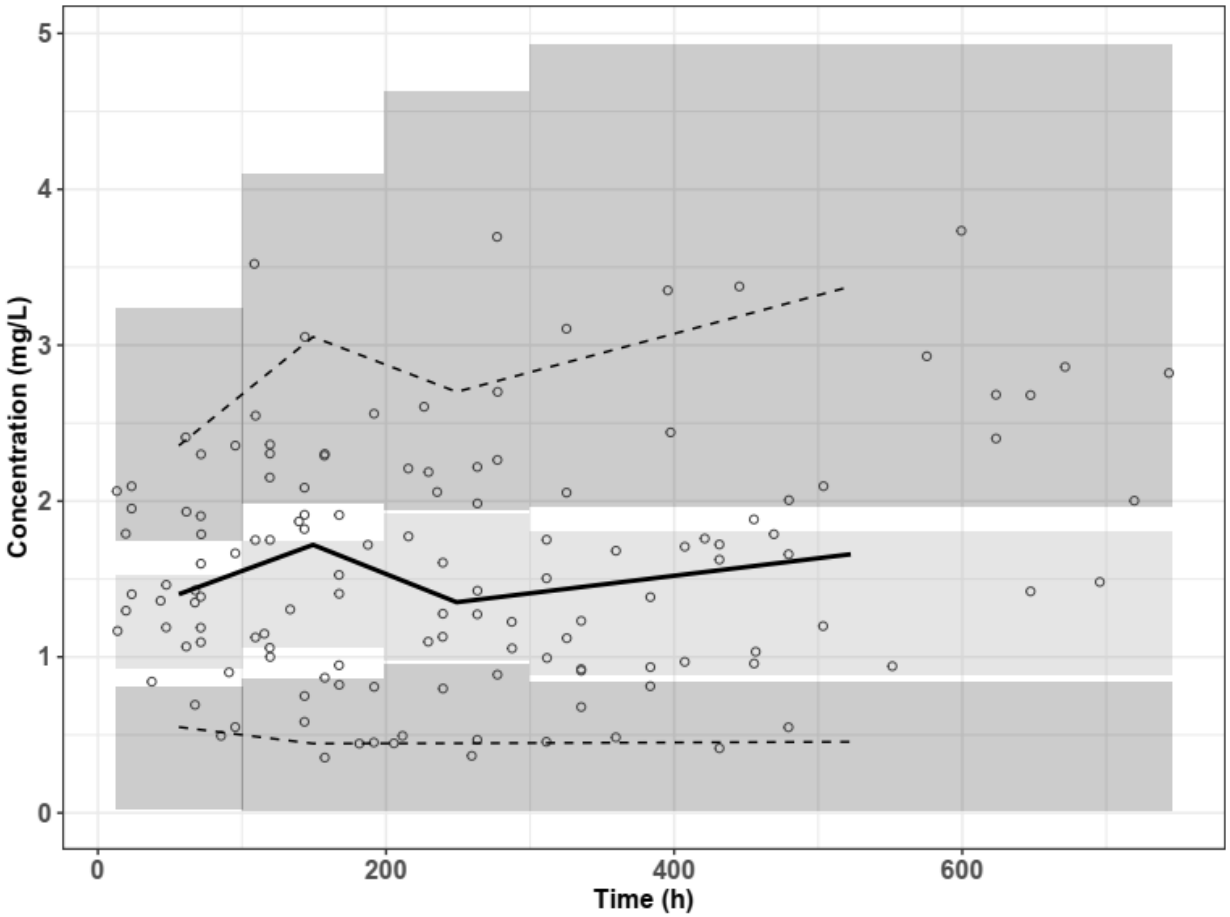

Figure 11. Prediction-corrected visual predicted check (pcVPC) of the final population pharmacokinetic model. The open circle represents the prediction-corrected vancomycin concentrations. Shaded areas show the 95% prediction interval of the 2.5th, 50^{th,} and 97.5th percentiles of the simulated values. The solid line indicates the observed median value. The upper and lower dashed lines are the observed 5th and 95th percentile values.

3.4. Simulation

PCZ PK profile was simulated following a 300 mg daily for one week. WT and total proteins levels consisted of the 5th, 50th, and 95th percentiles of the population distribution. The 50th percentile was used as a reference value for both WT and total proteins, while the absence of diarrhea was defined as the reference diarrhea status. The distribution of PCZ C_{min} at different covariates levels is shown in Figure 12. For a typical subject of 56 kg, total proteins level of 5.3 g/dL, and in the absence of diarrhea, the target exposure to PCZ was achieved by most patients

(82.6%). Additionally, simulation of C_{min} in the presence of diarrhea demonstrated that only 65.8% of the population reached the target of 0.7 mg/L, against 82.6% in the absence of diarrhea. Similarly, the PTA also appeared to be affected by varying levels of total proteins. The highest PTA was observed at normal total proteins level of 6.6 g/dl (94.6%), while the lowest PTA was achieved at the 5^{th} percentile of total proteins levels (49.3%). Furthermore, the results suggested that C_{min} is predicted to decrease with increasing WT. However, most patients reached acceptable PTA, except at higher 79kg. For which 74.4% of the population achieved the target exposure.

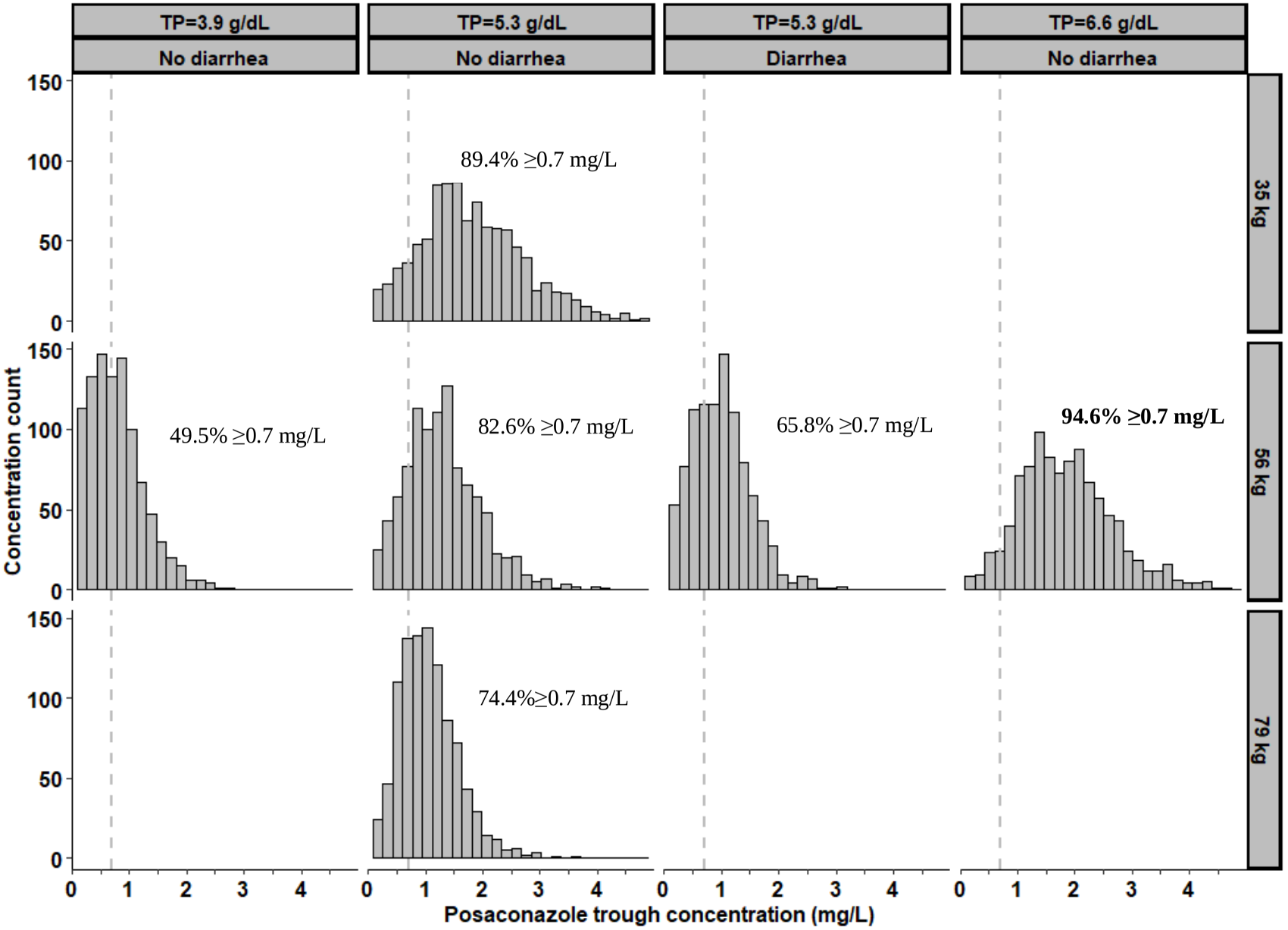
TP=3.9 g/dL
No diarrhea
TP=5.3 g/dL
No diarrhea
TP=5.3 g/dL
Diarrhea
TP=6.6 g/dL
No diarrhea
35 kg
56 kg
79 kg
89.4% ≥0.7 mg/L
49.5% ≥0.7 mg/L
82.6% ≥0.7 mg/L
65.8% ≥0.7 mg/L
94.6% ≥0.7 mg/L
74.4%≥0.7 mg/L
Concentration count
Posaconazole trough concentration (mg/L)

Figure 12. Distribution of posaconazole trough concentration (C_{min}) with varying covariates, following a dose of 300 mg for one week.

The dashed line represents the target exposure of 0.7 mg/dL.

TP, total proteins; WT, total body weight. Reference patient had a weight of 56 kg and total proteins level of 5.3 g/dL.

3.5. Safety assessment

From the 26 patients initially included in the PPK study, three patients with missing steady-state concentration were excluded from the safety analysis. Two patient showed elevation of LFTs during the second hospital admission on day 25 and 28, respectively. However, clinical data and PCZ exposure were missing during the discharge period. Therefore, the patients were also removed. A total of 21 patients were finally included, of which 47.6% (10/21) displayed LFTs abnormalities (38.5% in total, 10/26). For all patients, the levels of LFTs were reversible and moderately elevated (grade 2 or less). In addition, the increased LFTs were mostly AST and/or ALT (38%, n=8/21), while an elevation in ALP and TBIL was observed in one, and three patients, respectively. Among patients with LFTs abnormalities, three patients discontinued PCZ.

Other potential drug-induced AEs included fever (n=2), and nephrotoxicity (n=3).

Variables evaluated as potential predictors for hepatotoxicity included: sex, age, WT, baseline LFTs (ALT, AST, ALP, TBIL, ALBI score, and FIBI score), presence of cytomegalovirus (CMV), underlying malignancy, and HSCT status.

Kaplan-Meier curve for the cumulative incidence of hepatotoxicity is shown in Figure 13. The median time to occurrence of hepatotoxicity was 8.5 days, with the majority (80%) occurring within 14 days.

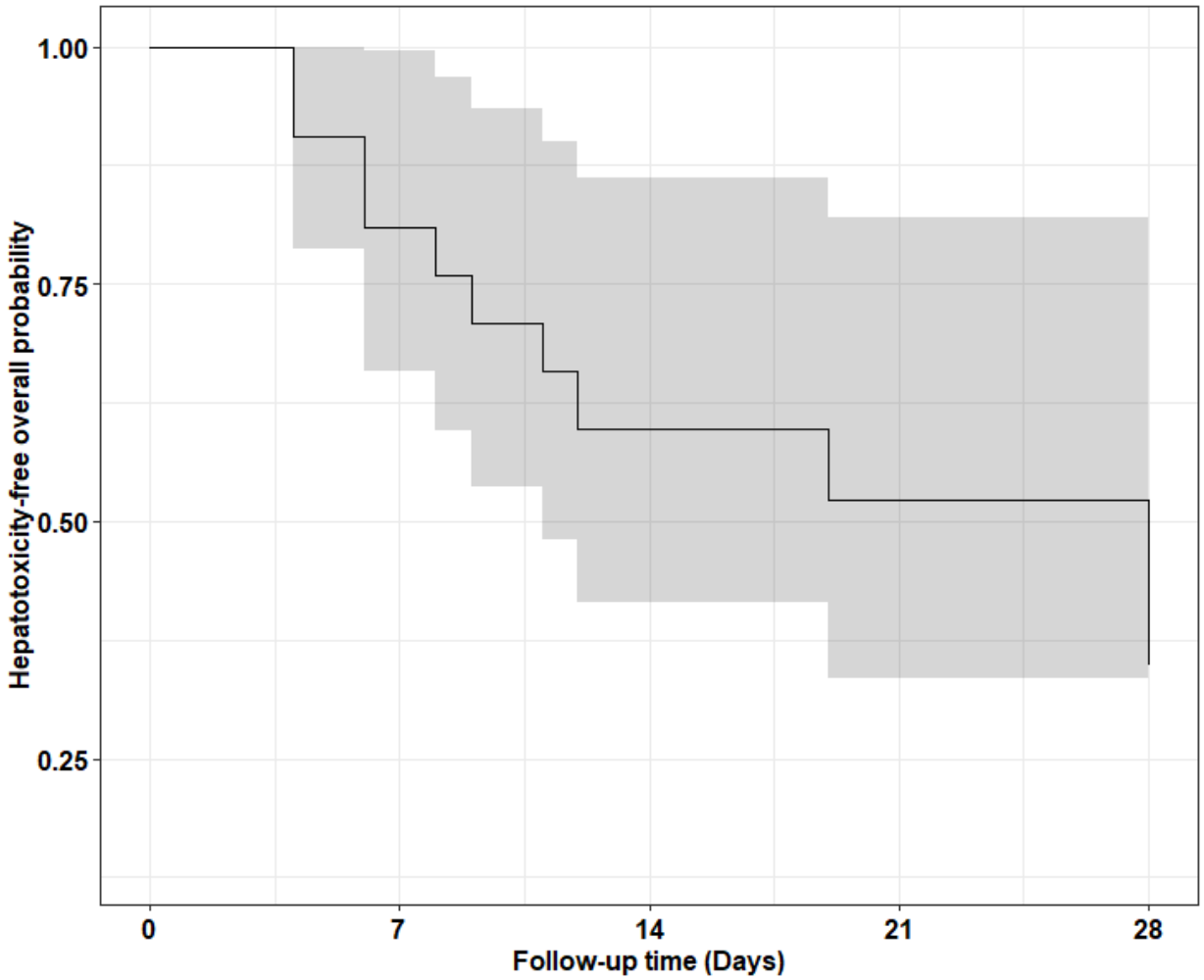

Figure 13. Kaplan-Meir curve for the cumulative probability of hepatotoxicity following posaconazole administration over a period of 28 days. Shaded area shows the 95% confidence interval.

As shown in Figure 14, PCZ C_{avr} was significantly different between patients with hepatotoxicity compared with patients without hepatotoxicity ($p < 0.05$). This was confirmed by the univariate analysis (Table 8), which demonstrated that PCZ C_{avr} and Age (≥65 years) were the only significant factors for hepatotoxicity. Multivariate cox regression analysis revealed that hepatotoxicity was independently associated with PCZ exposure, after adjusting for age (HR 4.7, $p < 0.05$; Table 8).

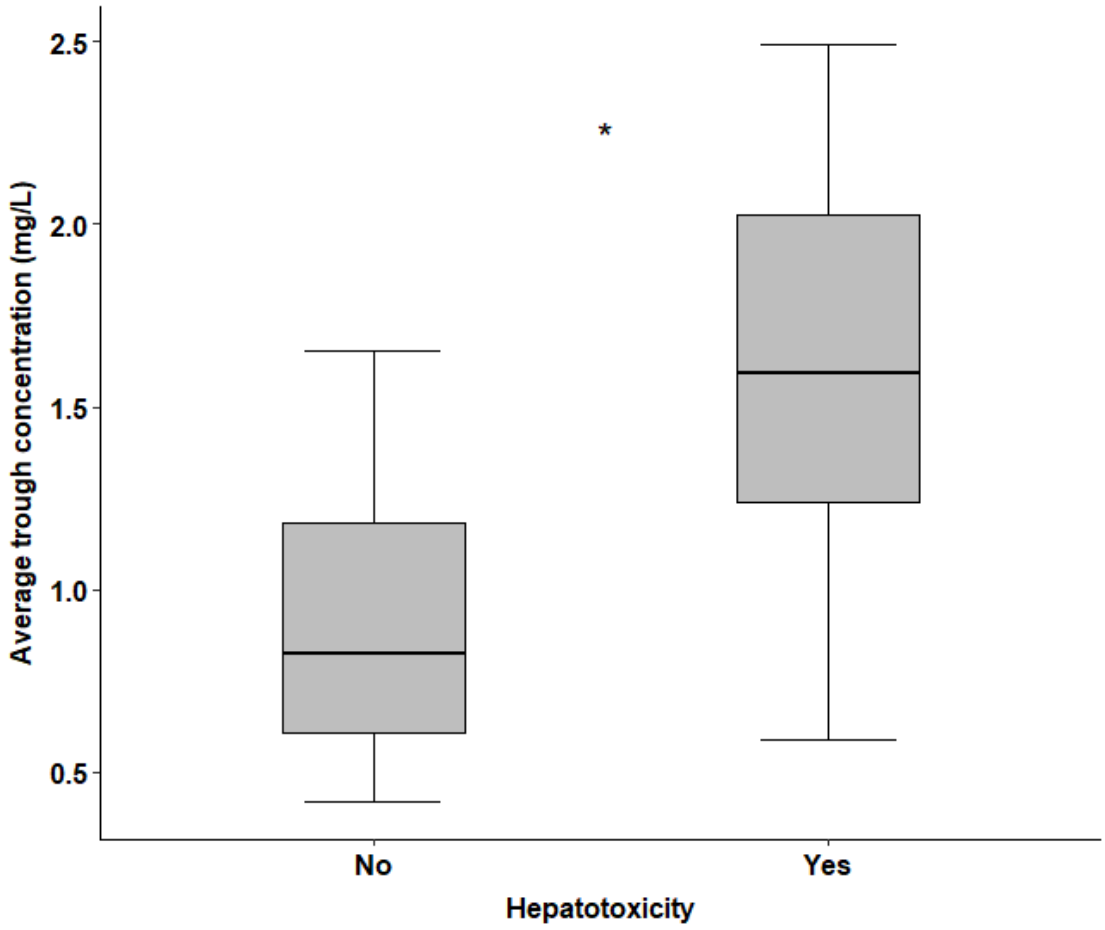

Figure 14. Comparison of posaconazole average trough concentration at steady-state between patients with hepatotoxicity and patients without hepatotoxicity. Limits of the box are the first and third quartiles corresponding to 25th and 75th percentiles, respectively. The lower and upper whiskers represent the minimum and maximum values without outliers.

* $p < 0.05$

Table 8. Summary of univariate and multivariate cox regression analysis

Characteristic	Univariate analysis		Multivariate analysis	
	HR (95% CI)	***p*-value**	**HR (95% CI)**	***p*-value**
Age (≥ 65 years)	5.8 (1.5–22)	**0.01***	5.8 (1.4–25.1)	**0.018***
Gender (Male vs. female)	1.1 (0.28–4.2)	0.9	-	-
Hematopoietic stem cell transplant	1 (0.21–4.9)	0.98	-	-
Cytomegalovirus	0.89 (0.19–4.2)	0.88	-	
Baseline ALBI score	2 (0.71–5.5)	0.2	-	-
Baseline ALBI grade III	2.9 (0.54–13)	0.23	-	-
Baseline FIB-4 score	1 (0.95–1.1)	0.42	-	-
Baseline FIB-4 grade III	0.38 (0.1–1.4)	0.14	-	-
Baseline aspartate aminotransferase	1 (0.94–1.1)	0.7	-	-
Baseline alanine aminotransferase	1 (0.98–1)	0.64	-	-
Baseline alkaline phosphatase	1 (1–1)	0.12	-	-
Baseline total bilirubin	2.9 (0.63–13)	0.17	-	-
AML and/or MDS	0.31 (0.085–1.2)	0.082	-	-
Posaconazole C_{avr}	5.1 (1.5–17)	**0.009** **	4.7 (1.4–15.5)	**0.012***

HR, hazard ratio; CI, confidence interval; ALBI, Albumin-Bilirubin; FIB-4, Fibrosis index, AML, Acute myeloid leukemia; MDS, Myelodysplastic syndrome; $C_{avr,}$ Posaconazole average concentration at steady state

** p <0.01; * p <0.05

4. Discussion

This study established a PPK model to characterize the PK and safety profile of PCZ DRT formulation in Japanese population with underlying hematologic malignancies. PCZ exposure was further shown to be associated with a higher risk of occurrence of hepatotoxicity. To our knowledge, this is the first study to investigate the relationship between PCZ trough concentration and elevation of LFTs, using a cox regression analysis. PCZ data were appropriately described by a one-compartment model with first-order absorption, which is consistent with existing PPK models.[98] The PCZ PK characteristics were also comparable to previous reports with the DRT formulation.[86,87,97] Based on the model, PCZ apparent CL/F was estimated to be 7.57 L/h/70kg, which was similar to two PPK models which reported values of values of 8.02 L/h, and 7.3 L/h, respectively.[86,99] Nevertheless, Vd in our model appeared to be lower, with an estimated value of 296 L/70kg against 548 L and 420 L, respectively.[86,99]

Previous PPK analyses have identified several influential covariates on the PK of PCZ OS.[98] However, the results of these studies are still conflicting and selected covariates are not always consistent. Possible reasons for this discrepancy include small sample size, limited data and variability in patients' characteristics. For instance, considering the lipophilic nature of PCZ, correlation between WT and PCZ clearance would be expected.[100,101] However, only few studies included WT as a covariate in their final model. Similarly, in our PPK model WT was found to improve the goodness of fit of the model, although not in a statistically significant manner. Simulation, demonstrated a limited clinical effect on PCZ exposure across lower levels of WT. However, PCZ trough was predicted to be lower at the 95th percentile, implying that dose adjustments may be necessary in patients with higher body weights

to achieve the desired therapeutic drug concentrations. Our results are in accordance with existing literature, suggesting higher risk of sub-therapeutic levels in obese patients.[75,81]

Among currently available PPK models for the DRT, only Pena-Lorenzo et al. included significant covariates on CL in the final model.[86] In their study, gender and total proteins were identified for the first time as significant covariates on CL/F. Consistent with these results, we have also found that PCZ CL/F was negatively affected by total proteins. These results were confirmed by the simulation analysis, which showed that the effect of total proteins on PCZ exposure was clinically relevant. This is not surprising, as PCZ is characterized by high protein binding (98 to 99%).[102]

Furthermore, according to a recent review of PCZ PPK models, the incidence of diarrhea was the most common covariate observed for the OS formulation.[98] However, a phase 3 study for the DRT formulation evaluated the effect of diarrhea but was not retained in the final model.[97] In our model, diarrhea was identified as a significant covariate associated with higher apparent CL/F. Additionally, the simulation results suggested that diarrhea could be clinically relevant on PCZ exposure.

Hepatotoxicity remains a major concern with fungal triazole use, particularly in patients with underlying liver disease or those receiving other potentially hepatotoxic medications.[103] Several studies have investigated the safety of PCZ DRT and has been found to be safe with low toxicity levels among patients. Moreover, the incidence of hepatotoxicity was not significantly different when compared to the OS, despite higher exposure profile.[68,71,74,88-90] Consistent with these results, no serious AEs were reported in our study, and were mostly mild to moderate. However, the incidence of hepatotoxicity in the present study (38.5%) was significantly higher compared to the

reported 15-20%.[80,90,91] Additionally, LFTs abnormality was the main reason for therapy discontinuation for most patients. The relationship between PCZ exposure and hepatotoxicity has been previously investigated but is yet to be clarified. A study by Van Iersel et al. found no correlation between increased plasma concentration of PCZ and liver toxicity.[97] Another study did not identify association between PCZ and elevation of LFTs but recommended that special attention should be paid when co-administered with hepatotoxic drugs.[87] Jia et al. on the other hand, found that plasma concentrations tended to be higher in patients with hepatotoxicity (1.83 ± 1.47 μg/mL) as compared with the patients without hepatotoxicity (1.2 ± 0.83 μg/mL), although these differences were not statistically significant ($P = 0.07$).[104] Notably, these studies were mainly descriptive, and the true relationship could have been missed. In contrast, we used for the first time a cox regression model to investigate the hazard for developing hepatotoxicity given PCZ exposure. The results of the multivariate analysis demonstrated that PCZ trough concentration significantly increased the probability of developing hepatotoxicity (HR 4.7, $p < 0.05$). Our results support Yang et al. meta-analysis finding, in which they evaluated the main AEs of currently used antifungal agents, and reported that PCZ was associated with the highest side effect rate when it comes to increase in liver enzymes and cardiac disorders.[103]

Our study does come with some limitations. First, the limited dataset and small sample size is likely to reduce the power for identifying significant covariates. Indeed, few covariates such as FIB-4 index grade 3 was found to be statistically significant, however 95% CI suggested limited information available. Second, although this analysis included several factors, it is possible that unrecognized confounders may have been missed. For example, the PK of PCZ are reportedly affected by the genetic polymorphism UGT1A4*3,[105] which may be associated with the higher IIV on CL in

our model. However, we could not investigate the potential effect of genetic polymorphism. Finally, due to the retrospective nature of the study, the follow-up period for the safety assessment was limited to 28 days, with most patients not reaching that target. In addition, hepatotoxicity in patients with hematologic malignancies may results from various factors. Therefore, to detect a drug-induced hepatotoxicity and exclude other possible causes related to the disease progression or concomitant drugs, a larger prospective study would be required.

5. Conclusions

PCZ PK have been successfully characterized using PPK modeling. In addition, PCZ exposure was found to be associated with a higher probability of developing hepatotoxicity. While PCZ DRT has been shown to be relatively safe, its safety profile with respect to hepatotoxicity remains a concern. Thus, LFTs should be monitored closely during PCZ therapy. The present findings have the potential to be used to better understand the incidence, mechanism, and management of PCZ-induced hepatotoxicity.

Chapter 3 Development and full validation of a bioanalytical method for quantifying letermovir in human plasma using ultra-performance liquid chromatography coupled with mass spectrometry

1. Introduction

Letermovir is a newly developed antiviral agent indicated in the prophylaxis of human CMV infections in adult recipients of HSCT.[106-108] Unlike other antiviral agents such as ganciclovir, foscarnet, and cidofovir, which target the viral DNA polymerase,[109] letermovir inhibits viral DNA cleavage by targeting the CMV terminase complex, pUL56.[110] It is commercially available in both intravenous and oral formulations with a recommended therapeutic dose of 480 mg once daily.[111]

Recently, several studies have reported various cases of CMV resistance during letermovir prophylaxis in HSCT recipients.[112-114] Furthermore, letermovir was found to increase tacrolimus exposure by inhibiting CYP3A4[115,116] and decrease voriconazole exposure in healthy recipients secondary to CYP2C9/19 induction.[117] It has also been found that co-administration with cyclosporine significantly decreases letermovir clearance, leading to an increase in letermovir exposure caused by the inhibitory effect of cyclosporine on OATP1B1/3 transporters; OATP1B1/3 is a hepatic metabolizer of letermovir.[116]

In light of these findings, further studies for assessing the PK and PD are required. However, although multiple clinical studies[108,115,116,118] mention the use of LC/MS methods for quantifying letermovir in human plasma, there is no information regarding the full method, including its validation in the available literature. More recently, a new method for the quantification of letermovir in human serum using HPLC combined with diode array detector has been published.[119] However, to date, no LC/MS method

has been described in human plasma. Thus, the main purpose of this work was to develop and validate an ultra-performance liquid chromatography (UPLC)/MS method for quantifying letermovir in human plasma, which is suitable for clinical studies as well as for therapeutic drug monitoring.

2. Materials and methods

2.1. Chemicals and reagents

The reference standard letermovir (≥98% purity) was purchased from Cayman Chemical (Ann Arbor, Michigan MI, USA). The chemical structure of letermovir is presented in Figure 15.[110] Roscovitine, which was used as the internal standard (IS), was purchased from Wako Pure Chemical Industries, Ltd. (Osaka, Japan). Methanol, acetonitrile, dimethylsulfoxide (DMSO, 99% purity), and formic acid (98% purity) were supplied by Wako Pure Chemical Industries, Ltd. (Osaka, Japan). Methanol and acetonitrile were both LC/MS grade. Ammonium formate (1 mol/L) and ammonium acetate (10 mol/L) were purchased from Nacalai Tesque, Inc. (Kyoto, Japan). Milli-Q water (of 18.2 mΩ) was obtained from an in-house purification system, Elga LabWater PURELAB® flex (Elga LabWater, High Wycombe, UK). Human blank plasma K2 dipotassium ethylenediaminetetraacetic acid (EDTA) was purchased from Cosmo Bio Co., Ltd. (Tokyo, Japan). Letermovir reference standard and human blank plasma were stored at −20°C prior to use.

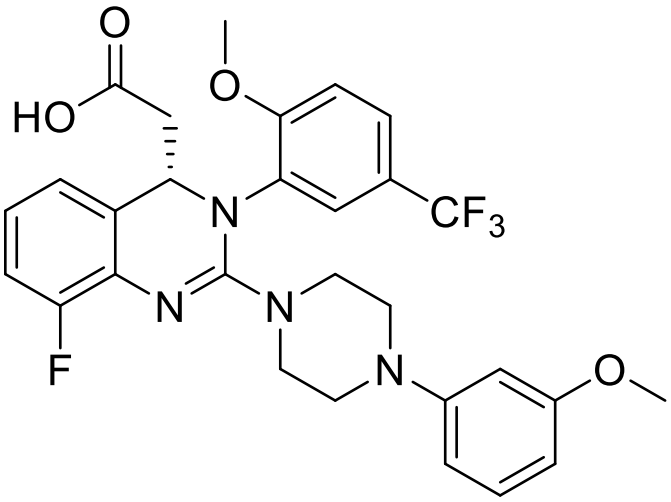

Figure 15. Chemical structure of letermovir ($C_{29}H_{28}F_4N_4O_4$).[110]

2.2. Equipment

The LC system consisted of an ACQUITY UPLC® system, equipped with an autosampler, a binary solvent manager, and an online degasser. Analyte separation was performed in reverse phase mode with an ACQUITY UPLC® BEH C18 column (130Å, 1.7 µm, 2.1 mm × 50 mm) preceded by Waters ACQUITY BEH C18 Van-Guard pre-column and detected using Waters ACQUITY® QDa detector. The chromatography system, column, and mass spectrometer were purchased from the Waters Corporation (Milford, MA, USA). Data manipulation was performed using the Empower 3 software (Waters Corporation, USA).

2.3. Method development

During method development, a large number of chromatographic and mass spectrophotometric parameters were screened and optimized by using a screening protocol, in order to develop a fast and robust bioanalytical method for quantifying letermovir in human plasma.

2.3.1. MS conditions

Detection of letermovir and IS, based on the peaks' mass to charge (*m/z*) ratio, was carried out using Waters ACQUITY® QDa detector through electrospray ionization operating in a positive ion mode. The cone and capillary voltages were 15 V and 0.8 kV, respectively. The probe temperature was set to 600°C, and the sampling rate was set to 10 points/sec.

2.3.2. Chromatographic conditions

Chromatographic separation was performed in reverse phase mode with an ACQUITY UPLC BEH C18 column maintained at 50°C. The mobile phase was delivered at a flow rate of 0.3 mL/min through gradient elution and consisted of 10 mM ammonium acetate in pure water with 0.1% formic acid added for pH adjustment (aqueous mobile phase A) and acetonitrile (organic mobile phase B). The total analytical run time for each injection was 6.1 min, including 2 min of re-equilibration.

The initial gradient conditions started with 10% mobile phase B which was maintained for 0.5 min. Mobile phase B was gradually increased to 40% over 1 min and further increased to 90% for 1.4 min. These conditions were held for 1.1 min, returned to initial conditions over 0.1 min, and maintained for 2 min. Optimization of chromatographic conditions involved the consecutive screening of the following parameters: buffer, pH of the mobile phase, organic solvent, gradient elution, flow rate, column temperature, and injection volume. The initial method conditions for the first screening were selected according to letermovir physicochemical properties (pKa values, molecular weight, solubility, and stability). The conditions offering the best retention and separation were then selected.

2.3.3. Samples preparation

Stock solution was prepared at 1 mg/mL by dissolving 5 mg of letermovir standard in DMSO. The stock solution was further diluted in an appropriate volume of methanol-water (1:1, v/v) to prepare a second stock solution at 100 µg/mL. From the second stock solution, two individual working solutions (calibration standard working solution and quality control (QC) working solutions) were freshly prepared in methanol-water (1:1, v/v) at 10 µg/mL and 7.5 µg/mL, respectively. Serial dilution with methanol-water (1:1, v/v) was then performed in order to obtain six calibration standard working solutions and three QC working solutions. The IS working solution was prepared at 5 µg/mL by diluting the corresponding stock solution in methanol-water (1:1, v/v).

2.3.4. Calibration standards, and QC samples

Calibration standard working solutions were diluted 10-fold with human blank plasma (1:9, v/v) to obtain six calibration standards at 10, 100, 200, 400, 800, and 1000 ng/mL. QC working solutions were also diluted 10-fold with human blank plasma to obtain QCs at three different concentration levels: i.e., low-, mid-, and high-: levels of 30, 500, and 750 ng/mL, respectively.

2.3.5. Samples pre-treatment

Ten microliters of the IS working solution were added to 1.5 mL centrifuge polyethylene tubes containing 100 µL of the corresponding calibration standard or QC diluted in human blank plasma. Protein precipitation was induced by adding 400 µL of methanol to all the samples. The tubes were vortexed for 1 min and centrifuged at 13000 g for 5 min. The supernatant was diluted with an appropriate volume of mobile phase (1:1, v/v), and 2 µL was injected into the LC/MS system.

2.4. Method validation

Full validation of the method in human plasma was performed in compliance with the FDA guidelines on bioanalytical method development and validation.[120] The validation included the following parameters: linearity and calibration curve, carry over, selectivity, intra- and inter- assay accuracy and precision, recovery and matrix effect, dilution linearity, and stability.

2.4.1. Linearity and calibration curve

Calibration standards were prepared at six concentrations over a range of 10–1000 ng/mL. Six individually prepared replicates at each concentration, including a blank and a zero calibrator standard (blank plasma spiked with IS), were analyzed within six different runs. In order to confirm the concentration-response relationship, calibration curves were plotted by fitting the peak response (*y*-axis), defined as the peak-area ratio of letermovir to IS, against the nominal concentration of the calibration standard (*x*-axis).

Concentrations were calculated using unweighted and weighted linear least-squares regression analysis with the weighting factors: 1, $1/x$, and $1/x^2$, where x is the concentration of letermovir. The choice of the weighting factor was based on the relationship between the standard deviation and variance of the LC/MS response and the analyte concentration.[121]

The coefficient of determination (R^2) should be ≥0.99. Accuracy (nominal%) and precision (relative standard deviation (RSD) %) at each concentration should be ± 15% and ≤15%, respectively, except at the lower limit of quantification (LLOQ), where the calculated concentration should be ± 20% of the nominal concentration and RSD ≤15%.

2.4.2. Carryover

Carryover was evaluated by analyzing a human blank plasma following the injection of an upper limit of quantification (ULOQ), the highest concentration calibration standard, in five different runs. Carryover should not exceed 20% of the LLOQ.

2.4.3. Selectivity

Selectivity was defined as the absence of substances interfering with the analyte and IS at the same retention time and was evaluated by analyzing six different human plasma samples prepared at LLOQ (10 ng/mL) and IS at 500 ng/mL. The human plasma samples should be free of interferences with the elution of the analyte and IS. If any peak is observed at the retention time of the analyte and/or IS, the response should be ≤20% of the LLOQ response and ≤5% of the response of the IS.

2.4.4. Accuracy and precision

Accuracy and precision were evaluated at LLOQ level, and with QCs prepared at three different concentrations. Repeatability or intra-assay accuracy, defined as nominal%, and precision (RSD%), were determined by analyzing five individually prepared replicates at each concentration within the same run and five injections of one replicate within another run to evaluate injection repeatability.

Inter-assay accuracy and precision were obtained by analyzing five individually prepared replicates at each concentration within five different days. Accuracy at each concentration level should be within ± 15%, and precision should be ≤15%, except at the LLOQ where accuracy and precision should be ± 20% and ≤20%, respectively.

2.4.5. Matrix effect and % recovery

QCs at low, mid, and high levels were prepared in six different human plasma samples. The matrix factor was evaluated by comparing the peak area of the QC prepared in human plasma with the peak area of the QC prepared in methanol-water (1:1, v/v).

Recovery was evaluated by comparing the peak area of the extracted QC prepared at three levels of concentration with the peak area of the extracted human plasma sample spiked with letermovir and IS at the same concentration. Precision expressed by the RSD% for both the matrix effect and recovery should not exceed 15%.

2.4.6. Dilution linearity

Plasma dilution in human blank plasma was assessed. Five individually prepared replicates of QCs at 10 times (10 µg/mL) the ULOQ were analyzed. The samples were diluted 10 times with human blank plasma to obtain samples of 1000 ng/mL. The mean accuracy at each level of concentration should be within ± 15%, and the precision expressed in RSD% should be ≤15%.

2.4.7. Stability

The stability of the stock solution was assessed by analyzing three individually prepared replicates in methanol-water (1:1, v/v) at 1 µg/mL, after storage at room temperature (RT, 24°C) for 6 h, and after storage at −20°C for 6 months and 12 months. The stability of letermovir in human blank plasma was determined using five individually prepared replicates of QCs at three concentration levels. The following stability conditions were assessed: short-term stability (24 h at RT and at −20°C), post-preparation (48 h at −20°C), auto-sampler (24 h at 10°C), freeze thaw (three cycles, −20°C/RT, and 24 h between cycles), and long-term stability (10 days at −20°C, and 30

days at −20°C and −80°C). Letermovir was considered stable under the different storage conditions if the accuracy (nominal%) and precision (RSD%) were within ± 15% and ≤ 15%, respectively.

3. Results

3.1. Method development

3.1.1. Mass spectrometry

The ionization conditions used in the full mass scan permitted the detection of prominent peaks for letermovir and IS with *m/z* of 573.30 and 355.31, respectively. Single chromatograms of letermovir were obtained by setting the QDa mass spectrometer to single *m/z* values previously obtained through a selected ion recording. The results of the full mass scan and SIR showed that no further optimization was required. Thus, initial ESI-MS was selected for optimizing the chromatographic conditions.

3.1.2. Liquid chromatography

The chromatographic method was optimized by changing various parameters such as pH of the buffer and organic solvent. Best separation, elution, and tailing were obtained with 10 mM ammonium acetate in pure water and 0.1% formic acid to obtain a pH of 5.2 (mobile phase A) and acetonitrile (mobile phase B). Furthermore, to achieve a capacity factor ≥2, the column temperature was maintained at 50°C and acetonitrile was gradually increased from 10% to 90%, over 2.9 min.

3.2. Method validation

3.2.1. Linearity and calibration curve

The equations of linear regression and coefficients of determination R^2 are described in Table 9. The concentration-response relationship was best described with a $1/x^2$ weighting factor. R^2 of six replicates was >0.99, and the accuracy of all six calibration points was within ± 15% of the nominal concentration. Thus, the calibration curve was validated over a range of 10–1000 ng/mL. The choice of the upper limit of 1000 ng/mL was based on the results of previous clinical trials.[108,116] The predicted median minimal concentration of letermovir in Asian patients after oral administration of 480 mg, and after oral administration of 240 mg with cyclosporine exposure were 506.4 ng/mL with a 90% prediction interval of 118.4–1628, and 1200 ng/mL with a 90% prediction interval of 346.9–3154, respectively.[108] Furthermore, according to a study conducted by Isberner et al., the median trough concentration of letermovir after oral administration of 240 mg or 480 mg in patients including children was 2603 ng/mL (range 175–12281 ng/mL), and two samples were less than 100 ng/mL. [122] These results suggest that letermovir concentrations exhibit a large variability in clinical setting. In this study, a lower ULOQ than that used in a previous study (5000 ng/mL) was chosen to improve the accuracy of our calibration curve, while a dilution integrity of 10-fold was assessed in order to account for concentrations above 1000 ng/mL.

Table 9. Calibration curve and regression parameters results obtained with unweighted and weighted linear regression analysis [a]

Weighting factor	Mean equation for regression line	Mean coefficient of determination (R^2)	Mean RE%[b]
1	$y = 0.000873\,x + 0.002119$	0.9995	−4.8
1/x	$y = 0.000879\,x - 0.000336$	0.9997	3.3×10^{-3}
$1/x^2$	$y = 0.000882\,x - 0.000484$	0.9995	5.0×10^{-2}

[a] Regression parameters obtained with calibration curves of six standards in six analytical runs

[b] Mean relative error (RE)%: ((obtained concentration − nominal concentration)/nominal concentration) × 100

3.2.2. Carry over

No response was detected in the five replicates of human blank plasma samples processed after a ULOQ sample at the retention time of letermovir and IS. Thus, no carry-over effect was observed.

3.2.3. Selectivity

The method showed good selectivity for letermovir and IS. The different chromatograms are presented in Figure 16. Retention times of letermovir and IS were 2.78 min and 2.69 min, respectively. No endogenous peak was observed in the human plasma samples at the retention times of letermovir and IS.

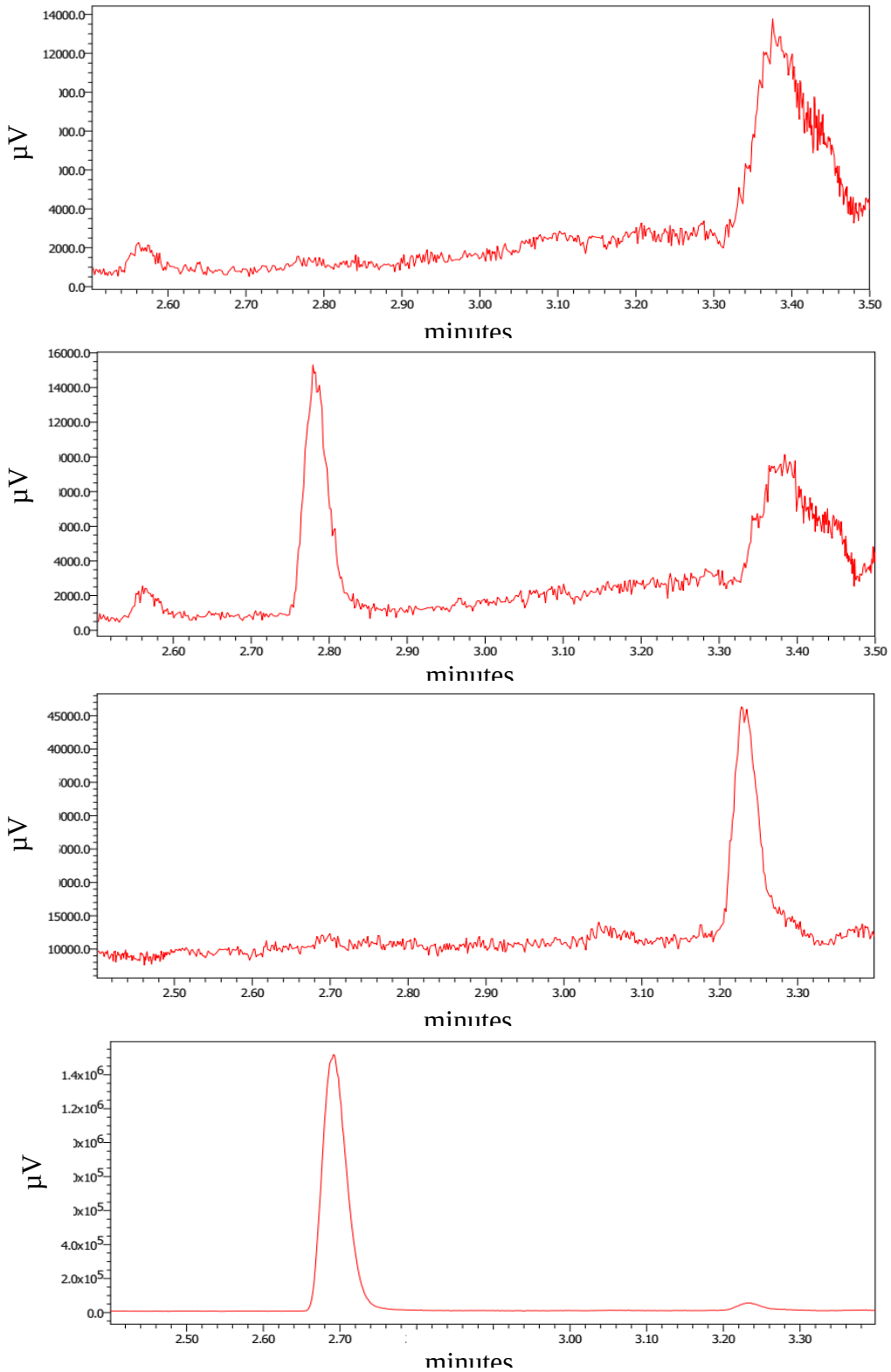

Figure 16. Chromatograms of letermovir and IS in human plasma; (A) Blank plasma *m/z* = 573.30; (B) Blank plasma spiked with letermovir at LLOQ (10 ng/mL); (C) Blank plasma *m/z* = 355.31; (D) Blank plasma spiked with IS (500 ng/mL).

3.2.4. Sensitivity

Sensitivity was evaluated with five LLOQ samples (10 ng/mL) as per the intra-assay accuracy and precision (Table 10). The results of the five replicates met the acceptance criteria of accuracy (nominal% ± 15%) and precision (RSD% ≤15%). %). The LLOQ determined in this assay (10 ng/mL) was lower than the LLOQ established in a previous study by Isberner et al. (100 ng/mL). [122]

3.2.5. Accuracy, precision, and dilution linearity

Table 10 summarizes the results of the intra-assay and inter-assay accuracy and precision. The accuracy of all the QCs at different levels was within ± 15%, and precision was ≤15%. Both the methods used in our study and in a previous study [122] conformed with the FDA guidelines for bioanalytical method validation, in terms of accuracy and precision.[120] Dilution linearity with human blank plasma was investigated at a ratio of 1:9. The mean accuracy and precision values obtained were 103% and 0.5%, respectively. All the results met the described acceptance criteria, suggesting that samples with a concentration >1000 ng/mL can be quantified with good accuracy and precision.

Table 10. Intra- and inter-assay accuracy and precision of letermovir QC samples

QC level	Nominal concentration (ng/mL)	Intra-assay (n = 5) [b]		Intra-assay (n = 5) [c]		Inter-assay (n = 5)	
		Accuracy (%)[a]	Precision (RSD%)	Accuracy (%)	Precision (RSD%)	Accuracy (%)	Precision (RSD%)
LLOQ	10	103	2.6	92	2.0	106	4.5
Low QC	30	99	3.3	110	1.2	99	3.0
Mid QC	500	101	1.9	108	0.4	100	3.6
High QC	750	102	1.7	106	0.4	100	2.3

LLOQ, lower limit of quantification; QC, quality control

[a] Accuracy: (obtained concentration/nominal concentration) × 100

[b] Five individually prepared replicates, [c] Five injections of one replicate

3.2.6. Matrix effect and recovery

The results of the matrix effect and extraction recoveries of letermovir and IS from human plasma samples are presented in Table 11. The mean extraction recoveries and RSD% at three levels of QCs were ± 15% and ≤15%, respectively, demonstrating a good recovery in different human plasma samples. The RSD% value of the matrix effect expressing the inter-subject variability was ≤15%. Furthermore, the RSD% of mean recovery and matrix effect of IS were also ≤15%. These results suggest that simple protein precipitation with methanol, compared to liquid−liquid extraction used by Isberner et al., [122] is efficient for pre-treatment of the samples and contributes to optimized sample preparation time while achieving a good recovery during extraction

Table 11. Matrix effect (n = 6) and recoveries of letermovir and IS from human plasma (n = 6)

	QC level	Nominal concentration (ng/mL)	Matrix effect		Recovery	
			Absolute matrix factor [a]	Precision (RSD%)	Recovery (%)[b]	Precision (RSD%)
Letermovir	Low QC	30	1.5	8.5	93	8.0
	Mid QC	500	1.3	4.0	97	4.8
	High QC	750	1.3	3.3	94	4.9
Roscovitine (IS)		500	1.0	5.4	101	5.7

QC, quality control

[a] Absolute matrix factor: (peak area of analyte in human plasma/peak area of analyte in neat solvent)

[b] Recovery%: (peak area of analyte in pre-spiked plasma/peak area of analyte in post-spiked plasma) × 100

3.2.7. Stability

The results of the stability studies are summarized in Tables 12. Letermovir stock solutions were stable for at least 1 year when prepared in a neat solvent. Furthermore, nominal% of QCs at three concentration levels after 30 days at −20°C and −80°C were within ± 15%. Thus, letermovir is stable for at least 30 days in human plasma under the described storage conditions.

Table 12. Stability results of letermovir in human plasma at different conditions (n = 5)

Stability condition	Nominal concentration (ng/mL)	Nominal[a] (%)	Precision (RSD%)
Auto sampler (10°C, 24 h)	30	106	2.3
	500	104	2.2
	750	103	1.4
Freeze-thaw	30	101	4.4
Three cycles (−20°C/RT, 24 h)	500	103	5.4
	750	105	3.2
Post-preparation (−20°C, 48 h)	30	102	3.7
	500	98	1.7
	750	94	2.0
Room temperature 24°C, 24 h	30	99	3.1
	500	99	3.6
	750	96	3.0
−20°C, 24 h	30	110	6.0
	500	102	4.3
	750	104	2.7
−20°C, 10 days	30	91	2.8
	500	96	1.7
	750	98	1.4
−20°C, 30 days	30	112	5.4
	500	111	2.6
	750	110	2.8
−80°C, 30 days	30	110	6.1
	500	110	2.3
	750	108	5.1

[a] Nominal% = (response at the stability condition/response of freshly prepared sample) × 100

RSD, residual standard error; RT, room temperature.

4. Discussion

The bioanalytical method developed and validated in this this study constitutes the first described LC/MS method for the quantification of letermovir in human plasma. The advantage of this method lies in its short analysis time of 6.1 min compared to 20 min in a previous HPLC assay with a retention time of 5.79 ± 0.15 min.[119] Furthermore, the method is characterized by a high sensitivity following the use of a mass spectrometer detector through a single ion recording, and is highly reproducible, owing to a sample preparation method.

The assay was fully validated with good selectivity and linearity over a large range of 10–1000 ng/mL. The choice of the upper limit of 1000 ng/mL was based on the results of previous clinical trials.[108,116] The predicted median minimal concentration of letermovir in Asian patients after oral administration of 480 mg, and after oral administration of 240 mg with cyclosporine exposure were 506.4 ng/mL with a 90% prediction interval of 118.4–1628, and 1200 ng/mL with a 90% prediction interval of 346.9–3154, respectively.[108] Furthermore, according to a study conducted by Isberner et al., the median trough concentration of letermovir after oral administration of 240 mg or 480 mg in patients including children was 2603 ng/mL (range 175–12281 ng/mL), and two samples were less than 100 ng/mL. [122] These results suggest that letermovir concentrations exhibit a large variability in clinical setting. In this study, a lower ULOQ than that used in a previous study (5000 ng/mL) was chosen to improve the accuracy of our calibration curve, while a dilution integrity of 10-fold was assessed in order to account for concentrations above 1000 ng/mL.

The results of the matrix effect and recovery suggest suggest that simple protein precipitation with methanol, compared to liquid−liquid extraction used by Isberner et al., [122] is efficient for pre-treatment of the samples and contributes to optimized sample

preparation time while achieving a good recovery during extraction. In addition, Letermovir was stable in neat solvent and plasma for at least 1 year and 30 days, respectively.

A limitation of this study is the absence of clinical application on plasma samples of patients receiving letermovir treatment. Thus, an assessment of the assay using patients' samples is required.

5. Conclusions

A rapid, simple, and sensitive LC/MS bioanalytical method for the quantification of letermovir in human plasma was developed and validated in accordance with FDA guidelines over a linear range of 10–1000 ng/mL. The method was successfully used to quantify letermovir in human plasma. This work could be useful to perform not only clinical PK/PD studies but also to investigate drug–drug interactions and letermovir side effects, which will be instructive in the creation of a dosage regimen and optimization of letermovir safety and efficiency.

Summary

Chapter 1 Population pharmacokinetic model and dosing optimization of vancomycin in hematologic malignancies with neutropenia and augmented renal clearance

Data on the pharmacokinetics (PK) and area under the curve (AUC) -based dosing strategy of vancomycin (VCM) in hematologic malignancies are limited. Therefore, we aimed to develop a population PK model, investigate the factors influencing VCM PK, and propose an optimal dosing regimen for hematologic malignancies.

A retrospective study was conducted in patients treated with VCM. A total of 148 patients were enrolled for population PK modeling. Simulation analyses were performed to identify dosing regimens achieving a target exposure of $AUC_{0\text{-}24}$ of 400–600 mg·h/L at the steady-state.

The VCM PK data were best described with a one-compartment model. Significant covariates included creatinine clearance (Ccr), diagnosis of acute myeloid leukemia (AML) and neutropenia on VCM clearance (CL), and body weight (WT) on the volume of distribution (Vd). The typical values of CL and Vd were 3.09 L/h (normalized to Ccr value of 90 mL/min) and 122 L/70 kg, respectively. Concerning the effect on VCM dosing, we found out that AML patients with neutropenia and ARC represent a critical population with a higher risk of VCM underexposure. Thus, individualized dosing adjustment and therapeutic drug monitoring are strongly recommended.

Chapter 2 Pharmacokinetics and safety evaluation of posaconazole delayed release table in hematologic malignancies

Limited information is available on the pharmacokinetics (PK) and safety of posaconazole (PCZ) delayed-release tablet. The aim of the study was to develop a population pharmacokinetic model, identify influential covariates, and investigate the relationship between PCZ exposure and hepatotoxicity.

A retrospective study was conducted in patients with underlying hematologic malignancies who received PCZ delayed-release tablets. A total of 26 patients were enrolled in the study.

PCZ data were adequately described by a one-compartment model with first-order absorption, using Nonlinear mixed effect modeling. Diarrhea and total proteins were identified as significant covariates on PCZ apparent clearance CL/F. The incidence of hepatotoxicity following PCZ therapy was 38.5% (10/26). For all patients, the levels of liver function tests (LFTs) were reversible and moderately elevated (grade 2 or less). Multivariate cox regression analysis revealed that hepatotoxicity was independently associated with older age (Hazard-ratio 5.8, p <0.05), and PCZ PCZ average trough concentration at steady-state (Hazard-ratio 4.7, p <0.05).

In this study, we characterized PCZ PK in Japanese population with hematologic malignancies, and identified total proteins as a significant covariate on PCZ apparent CL/F. In addition, this is the first study to identify PCZ trough concentration as an independent risk factor associated with higher risk for developing hepatotoxicity.

Chapter 3 Development and full validation of a bioanalytical method for quantifying letermovir in human plasma using ultra-performance liquid chromatography coupled with mass spectrometry

Letermovir is a newly developed antiviral agent indicated in the prophylaxis of human CMV infections in adult recipients of allogeneic hematopoietic stem cell transplants. Although multiple clinical studies mention the use of LC/MS, there is no information regarding the full method, including its validation in the available literature. Thus, the aim of this study was to develop and validate a rapid and simple ultra-performance liquid chromatography coupled with mass spectrometry (UPLC/MS) for the quantification of letermovir in human plasma.

Separation was performed in reverse phase mode using an ACQUITY UPLC BEH C18 column (130 Å, 1.7 µm, 2.1 mm × 50 mm) at a flow rate of 0.3 mL/min, 10 mM ammonium acetate-0.1% formic acid solution as mobile phase A, and acetonitrile as mobile phase B with a gradient elution. The method was validated over a linear range of 10–1000 ng/mL with a coefficient of determination (R^2) >0.99 using weighted linear regression analysis. The intra- and inter-assay accuracy (nominal%) and precision (relative standard deviation%) were within ± 15% and ≤15%, respectively. The specificity, recovery, matrix effect, stability, and dilution integrity of this method were also within acceptable limits.

This method constitutes the first described LC/MS method for the quantification of letermovir in human plasma, and could be used to perform not only clinical pharmacokinetics and pharmacodynamics studies but also to investigate drug–drug interactions and letermovir side effects.

Conclusion

In the present thesis, pharmacometrics approaches were successfully applied to characterize the PK and safety of an antibiotic, and an antifungal drug.

Through this work, we have demonstrated the importance of mathematical modeling and simulations in the optimization of antibiotics dosing to maximize efficacy and minimize the risk of toxicity. PK/PD modeling and simulation has a promising future in the battle against antimicrobial resistance. However, its full potential has yet to be fully integrated by clinicians, especially in hospital setting.

The field of model informed drug discovery is constantly evolving. Future research integrating not only pharmacometrics but also machine learning principles are strongly warranted and will undoubtedly play a significant role against the rapid spread of multidrug resistant pathogens.

References

1. WHO. Antimicrobial resistance: global report on surveillance 2014. 2014;

‹https://www.who.int/publications/i/item/9789241564748›, accessed December 2022.

2. CDC. Antibiotic Resistance Threats in the United States, 2019. Atlanta, GA: U.S. Department of Health and Human Services, CDC; 2019. 2019;doi:10.15620/cdc:82532

3. O'Neill J. Antimicrobial Resistance: Tackling a crisis for the health and wealth of nations. 2014;

‹https://amr-review.org/sites/default/files/AMR%20Review%20Paper%20-%20Tackling%20a%20crisis%20for%20the%20health%20and%20wealth%20of%20nations_1.pdf›, , accessed December 2022.

4. Naylor NR, Atun R, Zhu N, et al. Estimating the burden of antimicrobial resistance: a systematic literature review. *Antimicrob Resist Infect Control*. 2018;7:58. doi:10.1186/s13756-018-0336-y

5. Wozniak TM, Barnsbee L, Lee XJ, Pacella RE. Using the best available data to estimate the cost of antimicrobial resistance: a systematic review. *Antimicrob Resist Infect Control*. 2019;8:26. doi:10.1186/s13756-019-0472-z

6. Antimicrobial Resistance C. Global burden of bacterial antimicrobial resistance in 2019: a systematic analysis. *Lancet*. Feb 12 2022;399(10325):629-655. doi:10.1016/S0140-6736(21)02724-0

7. Bell BG, Schellevis F, Stobberingh E, Goossens H, Pringle M. A systematic review and meta-analysis of the effects of antibiotic consumption on antibiotic resistance. *BMC Infectious Diseases*. 2014/01/09 2014;14(1):13. doi:10.1186/1471-2334-14-13

8. Costelloe C, Metcalfe C, Lovering A, Mant D, Hay AD. Effect of antibiotic prescribing in primary care on antimicrobial resistance in individual patients: systematic review and meta-analysis. *BMJ*. May 18 2010;340:c2096. doi:10.1136/bmj.c2096

9. WHO. WHO guidelines on use of medically important antimicrobials in food-producing animals. Geneva: World Health Organization; 20. 2017; ‹https://apps.who.int/iris/bitstream/handle/10665/258970/9789241550130-eng.pdf?sequence=1›, December 2022

10. Pew. Tracking the Global Pipeline of Antibiotics in Development. ‹https://www.pewtrusts.org/en/research-and-analysis/issue-briefs/2019/09/tracking-the-global-pipeline-of-antibiotics-in-development› , accessed March 2023.

11. Owen JS, Fiedler-Kelly J. *Introduction to Population Pharmacokinetic / Pharmacodynamic*

Analysis with Nonlinear Mixed Effects Models. John Wiley & Sons, Inc. ; 2014.

12. Owens RC, Jr., Bulik CC, Andes DR. Pharmacokinetics-pharmacodynamics, computer decision support technologies, and antimicrobial stewardship: the compass and rudder. *Diagn Microbiol Infect Dis*. Aug 2018;91(4):371-382. doi:10.1016/j.diagmicrobio.2018.03.015

13. Trivedi A, Lee RE, Meibohm B. Applications of pharmacometrics in the clinical development and pharmacotherapy of anti-infectives. *Expert Rev Clin Pharmacol*. Mar 2013;6(2):159-70. doi:10.1586/ecp.13.6

14. Tsuji Y. Hospital Pharmacometrics for Optimal Individual Administration of Antimicrobial Agents for Anti-methicillin-resistant Staphylococcus aureus Infected Patients. *Biological and Pharmaceutical Bulletin*. 2021;44(9):1174-1183. doi:10.1248/bpb.b21-00002

15. Abdul-Aziz MH, Brady K, Cotta MO, Roberts JA. Therapeutic Drug Monitoring of Antibiotics: Defining the Therapeutic Range. *Ther Drug Monit*. Feb 1 2022;44(1):19-31. doi:10.1097/FTD.0000000000000940

16. de Velde F, Mouton JW, de Winter BCM, van Gelder T, Koch BCP. Clinical applications of population pharmacokinetic models of antibiotics: Challenges and perspectives. *Pharmacol Res*. Aug 2018;134:280-288. doi:10.1016/j.phrs.2018.07.005

17. Rybak MJ, Le J, Lodise TP, et al. Therapeutic monitoring of vancomycin for serious methicillin-resistant Staphylococcus aureus infections: A revised consensus guideline and review by the American Society of Health-System Pharmacists, the Infectious Diseases Society of America, the Pediatric Infectious Diseases Society, and the Society of Infectious Diseases Pharmacists. *Am J Health Syst Pharm*. May 19 2020;77(11):835-864. doi:http://doi.org/10.1093/ajhp/zxaa036

18. Hanai Y, Takahashi Y, Niwa T, et al. Clinical practice guidelines for therapeutic drug monitoring of teicoplanin: a consensus review by the Japanese Society of Chemotherapy and the Japanese Society of Therapeutic Drug Monitoring. *J Antimicrob Chemother*. Mar 31 2022;77(4):869-879. doi:10.1093/jac/dkab499

19. Haworth CS, Banks J, Capstick T, et al. British Thoracic Society guidelines for the management of non-tuberculous mycobacterial pulmonary disease (NTM-PD). *Thorax*. Nov 2017;72(Suppl 2):ii1-ii64. doi:10.1136/thoraxjnl-2017-210927

20. Gomez-Lopez A. Antifungal therapeutic drug monitoring: focus on drugs without a clear recommendation. *Clin Microbiol Infect*. Nov 2020;26(11):1481-1487. doi:10.1016/j.cmi.2020.05.037

21. Pappas PG, Kauffman CA, Andes DR, et al. Clinical Practice Guideline for the Management of Candidiasis: 2016 Update by the Infectious Diseases Society of America. *Clin Infect Dis*. Feb 15 2016;62(4):e1-50. doi:10.1093/cid/civ933

22. Patterson TF, Thompson GR, 3rd, Denning DW, et al. Practice Guidelines for the Diagnosis

and Management of Aspergillosis: 2016 Update by the Infectious Diseases Society of America. *Clin Infect Dis*. Aug 15 2016;63(4):e1-e60. doi:10.1093/cid/ciw326

23. Freifeld AG, Bow EJ, Sepkowitz KA, et al. Clinical practice guideline for the use of antimicrobial agents in neutropenic patients with cancer: 2010 update by the Infectious Diseases Society of America. *Clin Infect Dis*. Feb 15 2011;52(4):e56-93. doi:http://doi.org/10.1093/cid/cir073

24. Matsumoto K, Takesue Y, Ohmagari N, et al. Practice guidelines for therapeutic drug monitoring of vancomycin: a consensus review of the Japanese Society of Chemotherapy and the Japanese Society of Therapeutic Drug Monitoring. *J Infect Chemother*. Jun 2013;19(3):365-80. doi:http://doi.org/10.1007/s10156-013-0599-4

25. Rybak MJ, Lomaestro BM, Rotschafer JC, et al. Vancomycin therapeutic guidelines: a summary of consensus recommendations from the infectious diseases Society of America, the American Society of Health-System Pharmacists, and the Society of Infectious Diseases Pharmacists. *Clin Infect Dis*. Aug 1 2009;49(3):325-7. doi:http://doi.org/10.1086/600877

26. Fleming S, Yannakou CK, Haeusler GM, et al. Consensus guidelines for antifungal prophylaxis in haematological malignancy and haemopoietic stem cell transplantation, 2014. *Intern Med J*. Dec 2014;44(12b):1283-97. doi:http://doi.org/10.1111/imj.12595

27. Klastersky J. Management of Fever in Neutropenic Patients with Different Risks of Complications. *Clin Infect Dis*. 2004;39(1):S32-S37. doi:http://doi.org/10.1086/383050

28. Klastersky J, de Naurois J, Rolston K, et al. Management of febrile neutropaenia: ESMO Clinical Practice Guidelines. *Ann Oncol*. Sep 2016;27(suppl 5):v111-v118. doi:http://doi.org/10.1093/annonc/mdw325

29. Pagano L, Akova M, Dimopoulos G, Herbrecht R, Drgona L, Blijlevens N. Risk assessment and prognostic factors for mould-related diseases in immunocompromised patients. *J Antimicrob Chemother*. Jan 2011;66 Suppl 1:i5-14. doi:http://doi.org/10.1093/jac/dkq437

30. Zimmer AJ, Freifeld AG. Optimal Management of Neutropenic Fever in Patients With Cancer. *J Oncol Pract*. 2019;15(1):19-24. doi:http://doi.org/10.1200/JOP.18.00269

31. Lortholary O, Lefort A, Tod M, Chomat A-M, Darras-Joly C, Cordonnier C. Pharmacodynamics and pharmacokinetics of antibacterial drugs in the management of febrile neutropenia. *Lancet Inf Dis*. 2008;8(10):612-620. doi:http://doi.org/10.1016/s1473-3099(08)70228-7

32. Sime FB, Roberts MS, Warner MS, et al. Altered pharmacokinetics of piperacillin in febrile neutropenic patients with hematological malignancy. *Antimicrob Agents Chemother*. Jun 2014;58(6):3533-7. doi:http://doi.org/10.1128/AAC.02340-14

33. Theuretzbacher U. Pharmacokinetic and pharmacodynamic issues for antimicrobial therapy in patients with cancer. *Clin Infect Dis*. Jun 2012;54(12):1785-92.

doi:http://doi.org/10.1093/cid/cis210

34. Udy A, Roberts JA, Boots RJ, Paterson DL, Lipman J. Augmented renal clearance: implications for antibacterial dosing in the critically ill. *Clin pharmacokinet*. 2010;49(1):1-16. doi: http://doi.org/10.2165/11318140-000000000-00000

35. Baptista JP, Sousa E, Martins PJ, Pimentel JM. Augmented renal clearance in septic patients and implications for vancomycin optimisation. *Int J Antimicrob Agents*. May 2012;39(5):420-3. doi:http://doi.org/10.1016/j.ijantimicag.2011.12.011

36. Huttner A, Von Dach E, Renzoni A, et al. Augmented renal clearance, low beta-lactam concentrations and clinical outcomes in the critically ill: an observational prospective cohort study. *Int J Antimicrob Agents*. Apr 2015;45(4):385-92. doi:http://doi.org/10.1016/j.ijantimicag.2014.12.017

37. Johnston BW, Perry D, Habgood M, Joshi M, Krige A. Augmented renal clearance: a retrospective, cohort study of urinary creatinine clearance in critically ill patients in the United Kingdom. *J Int Med Res*. May 2021;49(5):3000605211015573. doi:http://doi.org/10.1177/03000605211015573

38. Minville V, Asehnoune K, Ruiz S, et al. Increased creatinine clearance in polytrauma patients with normal serum creatinine: a retrospective observational study. *Crit Care*. 2011;15(1):R49. doi:http://doi.org/10.1186/cc10013

39. Udy AA, Dulhunty JM, Roberts JA, et al. Association between augmented renal clearance and clinical outcomes in patients receiving beta-lactam antibiotic therapy by continuous or intermittent infusion: a nested cohort study of the BLING-II randomised, placebo-controlled, clinical trial. *Int J Antimicrob Agents*. May 2017;49(5):624-630. doi:http://doi.org/10.1016/j.ijantimicag.2016.12.022

40. Bilbao-Meseguer I, Rodriguez-Gascon A, Barrasa H, Isla A, Solinis MA. Augmented Renal Clearance in Critically Ill Patients: A Systematic Review. *Clin Pharmacokinet*. Sep 2018;57(9):1107-1121. doi:http://doi.org/10.1007/s40262-018-0636-7

41. Cook AM, Hatton-Kolpek J. Augmented Renal Clearance. *Pharmacotherapy*. Mar 2019;39(3):346-354. doi:http://doi.org/10.1002/phar.2231

42. Udy AA, Baptista JP, Lim NL, et al. Augmented renal clearance in the ICU: results of a multicenter observational study of renal function in critically ill patients with normal plasma creatinine concentrations*. *Crit Care Med*. Mar 2014;42(3):520-7. doi:http://doi.org/10.1097/CCM.0000000000000029

43. Udy AA, Lipman J, Jarrett P, et al. Are standard doses of piperacillin sufficient for critically ill patients with augmented creatinine clearance? *Crit Care*. Jan 30 2015;19:28. doi:http://doi.org/10.1186/s13054-015-0750-y

44. Udy AA, Varghese JM, Altukroni M, et al. Subtherapeutic initial beta-lactam concentrations

in select critically ill patients: association between augmented renal clearance and low trough drug concentrations. *Chest*. Jul 2012;142(1):30-39. doi:http://doi.org/10.1378/chest.11-1671

45. Chu Y, Luo Y, Ji S, Jiang M, Zhou B. Population pharmacokinetics of vancomycin in Chinese patients with augmented renal clearance. *J Infect Public Health*. Jan 2020;13(1):68-74. doi:http://doi.org/10.1016/j.jiph.2019.06.016

46. Izumisawa T, Kaneko T, Soma M, et al. Augmented Renal Clearance of Vancomycin in Hematologic Malignancy Patients. *Biol Pharm Bull*. 2019;42(12):2089-2094. doi:http://doi.org/10.1248/bpb.b19-00652

47. Minkute R, Briedis V, Steponaviciute R, Vitkauskiene A, Maciulaitis R. Augmented renal clearance--an evolving risk factor to consider during the treatment with vancomycin. *J Clin Pharm Ther*. Dec 2013;38(6):462-7. doi:http://doi.org/10.1111/jcpt.12088

48. Bury D, Ter Heine R, van de Garde EMW, Nijziel MR, Grouls RJ, Deenen MJ. The effect of neutropenia on the clinical pharmacokinetics of vancomycin in adults. *Eur J Clin Pharmacol*. Jul 2019;75(7):921-928. doi:http://doi.org/10.1007/s00228-019-02657-6

49. Choi MH, Choe YH, Lee SG, Jeong SH, Kim JH. Neutropenia is independently associated with sub-therapeutic serum concentration of vancomycin. *Clin Chim Acta*. Feb 2017;465:106-111. doi:http://doi.org/10.1016/j.cca.2016.12.021

50. Haeseker MB, Croes S, Neef C, Bruggeman CA, Stolk LM, Verbon A. Vancomycin Dosing in Neutropenic Patients. *PLoS ONE*. 2014;9(11)doi:http://doi.org/10.1371/journal.pone.0112008

51. Cockcroft DW, Gault MH. Prediction of Creatinine Clearance from Serum Creatinine. *Nephron*. 1976;16(1):31-41. doi:http://doi.org/10.1159/000180580

52. Health UDo, Services H. Common Terminology Criteria for Adverse Events. Accessed 21 April 2022, https://ctep.cancer.gov/protocoldevelopment/electronic_applications/docs/ctcae_v5_quick_reference_5x7.pdf

53. Abbot Co. L. ARCHITECT i Vancomycin. Accessed 14 April 2022, https://www.ilexmedical.com/files/PDF/Vancomycin_ARC.pdf

54. Bergstrand M, Hooker AC, Wallin JE, Karlsson MO. Prediction-corrected visual predictive checks for diagnosing nonlinear mixed-effects models. *AAPS J*. Jun 2011;13(2):143-51. doi:http://doi.org/10.1208/s12248-011-9255-z

55. Matsuo S, Imai E, Horio M, et al. Revised equations for estimated GFR from serum creatinine in Japan. *Am J Kidney Dis*. Jun 2009;53(6):982-92. doi:http://doi.org/10.1053/j.ajkd.2008.12.034

56. Hirai K, Ishii H, Shimoshikiryo T, et al. Augmented Renal Clearance in Patients With Febrile Neutropenia is Associated With Increased Risk for Subtherapeutic Concentrations of

Vancomycin. *Ther Drug Monit*. 2016;38(6):706-710. doi:http://doi.org/10.1097/FTD.0000000000000346

57. Binder S, Luciano M, Horejs-Hoeck J. The cytokine network in acute myeloid leukemia (AML): A focus on pro- and anti-inflammatory mediators. *Cytokine Growth Factor Rev*. Oct 2018;43:8-15. doi:http://doi.org/10.1016/j.cytogfr.2018.08.004

58. Carey A, Edwards DKt, Eide CA, et al. Identification of Interleukin-1 by Functional Screening as a Key Mediator of Cellular Expansion and Disease Progression in Acute Myeloid Leukemia. *Cell Rep*. Mar 28 2017;18(13):3204-3218. doi:http://doi.org/10.1016/j.celrep.2017.03.018

59. Recher C. Clinical Implications of Inflammation in Acute Myeloid Leukemia. *Front Oncol*. 2021;11:623952. doi:http://doi.org/10.3389/fonc.2021.623952

60. Kakihana Y, Ito T, Nakahara M, Yamaguchi K, Yasuda T. Sepsis-induced myocardial dysfunction: pathophysiology and management. *J Intensive Care*. 2016;4:22. doi:http://doi.org/10.1186/s40560-016-0148-1

61. Okada A, Kariya M, Irie K, et al. Population Pharmacokinetics of Vancomycin in Patients Undergoing Allogeneic Hematopoietic Stem-Cell Transplantation. *J Clin Pharmacol*. Sep 2018;58(9):1140-1149. doi:http://doi.org/10.1002/jcph.1106

62. Buelga DS, del Mar Fernandez de Gatta M, Herrera EV, Dominguez-Gil A, Garcia MJ. Population pharmacokinetic analysis of vancomycin in patients with hematological malignancies. *Antimicrob Agents Chemother*. Dec 2005;49(12):4934-41. doi:https://doi.org/10.1128/AAC.49.12.4934-4941.2005

63. Roberts JA, Taccone FS, Udy AA, Vincent JL, Jacobs F, Lipman J. Vancomycin dosing in critically ill patients: robust methods for improved continuous-infusion regimens. *Antimicrob Agents Chemother*. Jun 2011;55(6):2704-9. doi:http://doi.org/10.1128/AAC.01708-10

64. Del Mar Fernandez de Gatta Garcia M, Revilla N, Calvo MV, Dominguez-Gil A, Sanchez Navarro A. Pharmacokinetic/pharmacodynamic analysis of vancomycin in ICU patients. *Intensive Care Med*. Feb 2007;33(2):279-85. doi:http://doi.org/10.1007/s00134-006-0470-5

65. Hof H. A new, broad-spectrum azole antifungal: posaconazole--mechanisms of action and resistance, spectrum of activity. *Mycoses*. 2006;49 Suppl 1:2-6. doi:10.1111/j.1439-0507.2006.01295.x

66. Maertens JA, Girmenia C, Bruggemann RJ, et al. European guidelines for primary antifungal prophylaxis in adult haematology patients: summary of the updated recommendations from the European Conference on Infections in Leukaemia. *J Antimicrob Chemother*. Dec 1 2018;73(12):3221-3230. doi:10.1093/jac/dky286

67. Noxafil™ (posaconazole) [package insert]. package insert. 2015 . ‹https://www.accessdata.fda.gov/drugsatfda_docs/label/2015/022003s018s020,0205053s002s

004,0205596s001s003lbl.pdf›, accessed november 2020.

68. Kersemaekers WM, Dogterom P, Xu J, et al. Effect of a high-fat meal on the pharmacokinetics of 300-milligram posaconazole in a solid oral tablet formulation. *Antimicrob Agents Chemother*. 2015;59(6):3385-9. doi:10.1128/AAC.05000-14

69. Krishna G, Moton A, Ma L, Medlock MM, McLeod J. Pharmacokinetics and absorption of posaconazole oral suspension under various gastric conditions in healthy volunteers. *Antimicrob Agents Chemother*. Mar 2009;53(3):958-66. doi:10.1128/AAC.01034-08

70. Wong TY, Loo YS, Veettil SK, et al. Efficacy and safety of posaconazole for the prevention of invasive fungal infections in immunocompromised patients: a systematic review with meta-analysis and trial sequential analysis. *Sci Rep*. Sep 3 2020;10(1):14575. doi:10.1038/s41598-020-71571-0

71. Duarte RF, Lopez-Jimenez J, Cornely OA, et al. Phase 1b study of new posaconazole tablet for prevention of invasive fungal infections in high-risk patients with neutropenia. *Antimicrob Agents Chemother*. Oct 2014;58(10):5758-65. doi:10.1128/AAC.03050-14

72. Durani U, Tosh PK, Barreto JN, Estes LL, Jannetto PJ, Tande AJ. Retrospective Comparison of Posaconazole Levels in Patients Taking the Delayed-Release Tablet versus the Oral Suspension. *Antimicrob Agents Chemother*. Aug 2015;59(8):4914-8. doi:10.1128/AAC.00496-15

73. Kraft WK, Chang PS, van Iersel ML, Waskin H, Krishna G, Kersemaekers WM. Posaconazole tablet pharmacokinetics: lack of effect of concomitant medications altering gastric pH and gastric motility in healthy subjects. *Antimicrob Agents Chemother*. Jul 2014;58(7):4020-5. doi:10.1128/AAC.02448-13

74. Krishna G, Ma L, Martinho M, O'Mara E. Single-dose phase I study to evaluate the pharmacokinetics of posaconazole in new tablet and capsule formulations relative to oral suspension. *Antimicrob Agents Chemother*. Aug 2012;56(8):4196-201. doi:10.1128/AAC.00222-12

75. Miceli MH, Perissinotti AJ, Kauffman CA, Couriel DR. Serum posaconazole levels among haematological cancer patients taking extended release tablets is affected by body weight and diarrhoea: single centre retrospective analysis. *Mycoses*. Jul 2015;58(7):432-6. doi:10.1111/myc.12339

76. Vanstraelen K, Prattes J, Maertens J, et al. Posaconazole plasma exposure correlated to intestinal mucositis in allogeneic stem cell transplant patients. *Eur J Clin Pharmacol*. Aug 2016;72(8):953-63. doi:10.1007/s00228-016-2057-6

77. Krishna G, Ma L, Martinho M, Preston RA, O'Mara E. A new solid oral tablet formulation of posaconazole: a randomized clinical trial to investigate rising single- and multiple-dose pharmacokinetics and safety in healthy volunteers. *J Antimicrob Chemother*. Nov

2012;67(11):2725-30. doi:10.1093/jac/dks268

78. Pham AN, Bubalo JS, Lewis JS, 2nd. Comparison of posaconazole serum concentrations from haematological cancer patients on posaconazole tablet and oral suspension for treatment and prevention of invasive fungal infections. *Mycoses*. Apr 2016;59(4):226-233. doi:10.1111/myc.12452

79. Yi WM, Schoeppler KE, Jaeger J, et al. Voriconazole and posaconazole therapeutic drug monitoring: a retrospective study. *Ann Clin Microbiol Antimicrob*. Sep 11 2017;16(1):60. doi:10.1186/s12941-017-0235-8

80. Boglione-Kerrien C, Picard S, Tron C, et al. Safety study and therapeutic drug monitoring of the oral tablet formulation of posaconazole in patients with haematological malignancies. *J Cancer Res Clin Oncol*. Jan 2018;144(1):127-134. doi:10.1007/s00432-017-2523-2

81. Martson AG, Veringa A, Bakker M, et al. Posaconazole trough concentrations are not influenced by inflammation: A prospective study. *Int J Antimicrob Agents*. Mar 2019;53(3):325-329. doi:10.1016/j.ijantimicag.2019.01.006

82. Gautier-Veyret E, Bolcato L, Roustit M, et al. Treatment by Posaconazole Tablets, Compared to Posaconazole Suspension, Does Not Reduce Variability of Posaconazole Trough Concentrations. *Antimicrob Agents Chemother*. Oct 2019;63(10)doi:10.1128/aac.00484-19

83. Martson AG, Veringa A, van den Heuvel ER, et al. Posaconazole therapeutic drug monitoring in clinical practice and longitudinal analysis of the effect of routine laboratory measurements on posaconazole concentrations. *Mycoses*. Aug 2019;62(8):698-705. doi:10.1111/myc.12948

84. Prayag PS, Panchakshari SP, Mahalle NP, et al. Factors associated with subtherapeutic levels of oral posaconazole tablet: a detailed analysis from a tertiary care center in India. *Int J Infect Dis*. Nov 2022;124:76-80. doi:10.1016/j.ijid.2022.09.004

85. Jansen AME, Muilwijk EW, van der Velden W, et al. Posaconazole bioavailability of the solid oral tablet is reduced during severe intestinal mucositis. *Clin Microbiol Infect*. Jul 2022;28(7):1003-1009. doi:10.1016/j.cmi.2022.01.029

86. Pena-Lorenzo D, Rebollo N, Sanchez-Hernandez JG, et al. Population pharmacokinetics of a posaconazole tablet formulation in transplant adult allogeneic stem cell recipients. *Eur J Pharm Sci*. Jan 1 2022;168:106049. doi:10.1016/j.ejps.2021.106049

87. Petitcollin A, Boglione-Kerrien C, Tron C, et al. Population Pharmacokinetics of Posaconazole Tablets and Monte Carlo Simulations To Determine whether All Patients Should Receive the Same Dose. *Antimicrob Agents Chemother*. Nov 2017;61(11)doi:10.1128/AAC.01166-17

88. Cornely OA, Duarte RF, Haider S, et al. Phase 3 pharmacokinetics and safety study of a posaconazole tablet formulation in patients at risk for invasive fungal disease. *J Antimicrob*

Chemother. Mar 2016;71(3):718-26. doi:10.1093/jac/dkv380

89. Pham AN, Bubalo JS, Lewis JS, 2nd. Posaconazole Tablet Formulation at 400 Milligrams Daily Achieves Desired Minimum Serum Concentrations in Adult Patients with a Hematologic Malignancy or Stem Cell Transplant. *Antimicrob Agents Chemother*. Nov 2016;60(11):6945-6947. doi:10.1128/AAC.01489-16

90. Fortun J, Gioia F, Cardozo C, et al. Posaconazole salvage therapy: The Posifi study. *Mycoses*. Jun 2019;62(6):526-533. doi:10.1111/myc.12911

91. Tverdek FP, Heo ST, Aitken SL, Granwehr B, Kontoyiannis DP. Real-Life Assessment of the Safety and Effectiveness of the New Tablet and Intravenous Formulations of Posaconazole in the Prophylaxis of Invasive Fungal Infections via Analysis of 343 Courses. *Antimicrob Agents Chemother*. Aug 2017;61(8)doi:10.1128/AAC.00188-17

92. Shah AG, Lydecker A, Murray K, et al. Comparison of noninvasive markers of fibrosis in patients with nonalcoholic fatty liver disease. *Clin Gastroenterol Hepatol*. Oct 2009;7(10):1104-12. doi:10.1016/j.cgh.2009.05.033

93. Johnson PJ, Berhane S, Kagebayashi C, et al. Assessment of Liver Function in Patients With Hepatocellular Carcinoma: A New Evidence-Based Approach—The ALBI Grade. *Journal of Clinical Oncology*. 2015;33(6):550-558. doi:10.1200/jco.2014.57.9151

94. Hiraoka A, Michitaka K, Kumada T, et al. Validation and Potential of Albumin-Bilirubin Grade and Prognostication in a Nationwide Survey of 46,681 Hepatocellular Carcinoma Patients in Japan: The Need for a More Detailed Evaluation of Hepatic Function. *Liver Cancer*. Nov 2017;6(4):325-336. doi:10.1159/000479984

95. Chumpitazi BP, Self MM, Czyzewski DI, Cejka S, Swank PR, Shulman RJ. Bristol Stool Form Scale reliability and agreement decreases when determining Rome III stool form designations. *Neurogastroenterol Motil*. Mar 2016;28(3):443-8. doi:10.1111/nmo.12738

96. Ullmann AJ, Aguado JM, Arikan-Akdagli S, et al. Diagnosis and management of Aspergillus diseases: executive summary of the 2017 ESCMID-ECMM-ERS guideline. *Clin Microbiol Infect*. May 2018;24 Suppl 1:e1-e38. doi:10.1016/j.cmi.2018.01.002

97. van Iersel M, Rossenu S, de Greef R, Waskin H. A Population Pharmacokinetic Model for a Solid Oral Tablet Formulation of Posaconazole. *Antimicrob Agents Chemother*. Jul 2018;62(7)doi:10.1128/AAC.02465-17

98. Ding Q, Huang S, Sun Z, Chen K, Li X, Pei Q. A Review of Population Pharmacokinetic Models of Posaconazole. *Drug Des Devel Ther*. 2022;16:3691-3709. doi:10.2147/DDDT.S384637

99. Pettit NN, Miceli MH, Rivera CG, et al. Multicentre study of posaconazole delayed-release tablet serum level and association with hepatotoxicity and QTc prolongation. *J Antimicrob Chemother*. Aug 1 2017;72(8):2355-2358. doi:10.1093/jac/dkx122

100. Vehreschild JJ, Muller C, Farowski F, et al. Factors influencing the pharmacokinetics of prophylactic posaconazole oral suspension in patients with acute myeloid leukemia or myelodysplastic syndrome. *Eur J Clin Pharmacol*. Jun 2012;68(6):987-95. doi:10.1007/s00228-012-1212-y

101. Wasmann RE, Smit C, van Donselaar MH, et al. Implications for IV posaconazole dosing in the era of obesity. *J Antimicrob Chemother*. Apr 1 2020;75(4):1006-1013. doi:10.1093/jac/dkz546

102. Chen L, Krekels EHJ, Verweij PE, Buil JB, Knibbe CAJ, Bruggemann RJM. Pharmacokinetics and Pharmacodynamics of Posaconazole. *Drugs*. May 2020;80(7):671-695. doi:10.1007/s40265-020-01306-y

103. Yang YL, Xiang ZJ, Yang JH, Wang WJ, Xu ZC, Xiang RL. Adverse Effects Associated With Currently Commonly Used Antifungal Agents: A Network Meta-Analysis and Systematic Review. *Front Pharmacol*. 2021;12:697330. doi:10.3389/fphar.2021.697330

104. Jia MM, Zhang QW, Qin ZF, et al. Deciphering the Relationship Between the Trough Concentration of Posaconazole and Its Efficacy and Safety in Chinese Patients With Hematological Disorders. *Front Pharmacol*. 2020;11:575463. doi:10.3389/fphar.2020.575463

105. Suh HJ, Yoon SH, Yu KS, et al. The Genetic Polymorphism UGT1A4*3 Is Associated with Low Posaconazole Plasma Concentrations in Hematological Malignancy Patients Receiving the Oral Suspension. *Antimicrob Agents Chemother*. Jul 2018;62(7)doi:10.1128/aac.02230-17

106. Chemaly RF, Ullmann AJ, Stoelben S, et al. *N Engl J Med*. May 8 2014;370(19):1781-9. doi:10.1056/NEJMoa1309533

107. Goldner T, Hewlett G, Ettischer N, Ruebsamen-Schaeff H, Zimmermann H, Lischka P. The novel anticytomegalovirus compound AIC246 (Letermovir) inhibits human cytomegalovirus replication through a specific antiviral mechanism that involves the viral terminase. *J Virol*. Oct 2011;85(20):10884-93. doi:10.1128/JVI.05265-11

108. Marty FM, Ljungman P, Chemaly RF, et al. Letermovir Prophylaxis for Cytomegalovirus in Hematopoietic-Cell Transplantation. *N Engl J Med*. Dec 21 2017;377(25):2433-2444. doi:10.1056/NEJMoa1706640

109. Schreiber A, Harter G, Schubert A, Bunjes D, Mertens T, Michel D. Antiviral

treatment of cytomegalovirus infection and resistant strains. Expert Opin

Pharmacother. *Expert Opin Pharmacother*. 2009;10:191-209.

110. Lischka P, Hewlett G, Wunberg T, et al. In vitro and in vivo activities of the novel anticytomegalovirus compound AIC246. *Antimicrob Agents Chemother*. Mar 2010;54(3):1290-7. doi:10.1128/AAC.01596-09

111. PREVYMIS™ (letermovir) [package insert]. package insert. 2017 . ‹https://www.accessdata.fda.gov/drugsatfda_docs/label/2019/209939s005,209940s003lbl.pdf›,

accessed november 2019.

112. Frietsch JJ, Michel D, Stamminger T, et al. In Vivo Emergence of UL56 C325Y Cytomegalovirus Resistance to Letermovir in a Patient with Acute Myeloid Leukemia after Hematopoietic Cell Transplantation. *Mediterr J Hematol Infect Dis*. 2019;11(1):e2019001. doi:10.4084/MJHID.2019.001

113. Jung S, Michel M, Stamminger T, Michel D. Fast breakthrough of resistant cytomegalovirus during secondary letermovir prophylaxis in a hematopoietic stem cell transplant recipient. *BMC Infect Dis*. May 8 2019;19(1):388. doi:10.1186/s12879-019-4016-1

114. Komatsu TE, Hodowanec AC, Colberg-Poley AM, et al. In-depth genomic analyses identified novel letermovir resistance-associated substitutions in the cytomegalovirus UL56 and UL89 gene products. *Antiviral Res*. Sep 2019;169:104549. doi:10.1016/j.antiviral.2019.104549

115. Kropeit D, von Richter O, Stobernack HP, Rubsamen-Schaeff H, Zimmermann H. Pharmacokinetics and Safety of Letermovir Coadministered With Cyclosporine A or Tacrolimus in Healthy Subjects. *Clin Pharmacol Drug Dev*. Jan 2018;7(1):9-21. doi:10.1002/cpdd.388

116. McCrea JB, Macha S, Adedoyin A, et al. Pharmacokinetic Drug-Drug Interactions Between Letermovir and the Immunosuppressants Cyclosporine, Tacrolimus, Sirolimus, and Mycophenolate Mofetil. *J Clin Pharmacol*. Oct 2019;59(10):1331-1339. doi:10.1002/jcph.1423

117. Marshall WL, McCrea JB, Macha S, et al. Pharmacokinetics and Tolerability of Letermovir Coadministered With Azole Antifungals (Posaconazole or Voriconazole) in Healthy Subjects. *J Clin Pharmacol*. Jul 2018;58(7):897-904. doi:10.1002/jcph.1094

118. Kropeit D, Scheuenpflug J, Erb-Zohar K, et al. Pharmacokinetics and safety of letermovir, a novel anti-human cytomegalovirus drug, in patients with renal impairment. *Br J Clin Pharmacol*. Sep 2017;83(9):1944-1953. doi:10.1111/bcp.13292

119. Isberner N, Aghai F, Schirmer D, Kraus S, Grigoleit GU, Klinker H. Quantification of letermovir in human serum using high-performance liquid chromatography with diode array detection. *J Chromatogr B Analyt Technol Biomed Life Sci*. Nov 30 2020;1159:122399. doi:10.1016/j.jchromb.2020.122399

120. U.S. Department of Health and Human Services, Food and Drug Admnistration, (CDER). *"Guidance for industry: Bioanalytical method validation."*. May 2018: ‹https://www.fda.gov/downloads/Drugs/GuidanceComplianceRegulatoryInformation/Guidances/ucm070107.pdf›, accessed 10 October, 2019

121. Gu H, Liu G, Wang J, Aubry AF, Arnold ME. Selecting the correct weighting factors for linear and quadratic calibration curves with least-squares regression algorithm in bioanalytical

LC-MS/MS assays and impacts of using incorrect weighting factors on curve stability, data quality, and assay performance. *Anal Chem*. Sep 16 2014;86(18):8959-66. doi:10.1021/ac5018265

122. Isberner N, Aghai F, Schirmer D, Kraus S, Grigoleit GU, Klinker H. Quantification of letermovir in human serum using high-performance liquid chromatography with diode array detection. *J Chromatogr B Analyt Technol Biomed Life Sci*. Nov 30 2020;1159:122399. doi:10.1016/j.jchromb.2020.122399

Paper list

1. Population pharmacokinetic model and dosing optimization of vancomycin in hematologic malignancies with neutropenia and augmented renal clearance.

   Tassadit Belabbas, Takaaki Yamada, Nobuaki Egashira, Takeshi Hirota, Kimitaka Suetsugu, Yasuo Mori, Koji Kato, Koichi Akashi, Ichiro Ieiri
   J Infect Chemother. 2023;29(4):391-400.

2. Pharmacokinetics and safety evaluation of posaconazole delayed-release table in hematologic malignancies.
   Preparing for submission.

3. Development and Full Validation of a Bioanalytical Method for Quantifying Letermovir in Human Plasma Using Ultra-Performance Liquid Chromatography Coupled with Mass Spectrometry.

   Tassadit Belabbas, Takaaki Yamada, Yuichi Tsuchiya, Kimitaka Suetsugu, Nobuaki Egashira, and Ichiro Ieiri
   Chem. Pharm. Bull. 69, 646–651 (2021)

Acknowledgment

First and foremost, I would like to express my sincere gratitude to Prof. Ieiri and Dr. Egashira for their unlimited support, consideration, and unconditional guidance during my PhD journey.

I extend my deepest appreciation to Dr. Yamada, who guided and instructed me for the past four years. Without your assistance, expertise, invaluable advice, and dedicated involvement in every step, this thesis would not have been accomplished.

I also wish to thank Dr. Hirota, for his constructive feedback, insightful comments and enriching discussions to help make this thesis as good as it can be.

I thank MEXT for making my Ph.D in Japan possible. It has been an honor to be a recipient of this prestigious scholarship, and my time studying and living in Japan has been truly rewarding.

Last but not least, I would like to thank my family for all their love and encouragement. Thank you for always being so supportive and helping in every step of the way even from thousands of miles away.